© 2014. Published by The Company of Biologists Ltd | Journal of Cell Science (2014) 127, 4833–4845 doi:10.1242/jcs.146977

RESEARCH ARTICLE

Enrichment of the β-catenin–TCF complex at the S and G2 phases ensures cell survival and cell cycle progression

Yajie Ding[1,*], Shang Su[1,*], Weixin Tang[1], Xiaolei Zhang[1], Shengyao Chen[1], Guixin Zhu[1], Juan Liang[1], Wensheng Wei[2], Ye Guo[3], Lei Liu[3], Ye-Guang Chen[4] and Wei Wu[1,‡]

ABSTRACT

Wnt–β-catenin (β-catenin is also known as CTNNB1 in human) signaling through the β-catenin–TCF complex plays crucial roles in tissue homeostasis. Wnt-stimulated β-catenin–TCF complex accumulation in the nucleus regulates cell survival, proliferation and differentiation through the transcription of target genes. Compared with their levels in G1, activation of the receptor LRP6 and cytosolic β-catenin are both upregulated in G2 cells. However, accumulation of the Wnt pathway negative regulator AXIN2 also occurs in this phase. Therefore, it is unclear whether Wnt signaling is active in G2 phase cells. Here, we established a bimolecular fluorescence complementation (BiFC) biosensor system for the direct visualization of the β-catenin–TCF interaction in living cells. Using the BiFC biosensor and co-immunoprecipitation experiments, we demonstrate that levels of the nucleus-localized β-catenin–TCF complex increase during the S and G2 phases, and declines in the next G1 phase. Accordingly, a subset of Wnt target genes is transcribed by the β-catenin–TCF complex during both the S and G2 phases. By contrast, transient inhibition of this complex disturbs both cell survival and G2/M progression. Our results suggest that in S and G2 phase cells, Wnt–β-catenin signaling is highly active and functions to ensure cell survival and cell cycle progression.

KEY WORDS: Cell cycle, β-catenin, TCF, BiFC, Cell survival

INTRODUCTION

Canonical Wnt–β-catenin (β-catenin is also known as CTNNB1 in human) signaling functions in multiple developmental events during embryogenesis and in adult tissue homeostasis and carcinogenesis (Logan and Nusse, 2004; Moon et al., 2004; Klaus and Birchmeier, 2008; Clevers and Nusse, 2012). In the absence of Wnt ligands, levels of cytoplasmic β-catenin are fine tuned through the 'destruction complex'. This complex includes tumor suppressor adenomatous polyposis coli (APC), the central scaffold protein Axin, glycogen synthase kinase 3β (GSK3β) and casein kinase 1 (CK1) as the core components (MacDonald et al., 2009). β-catenin is phosphorylated at the N-terminus by CK1 at residue S45 and by GSK3β at residues S33, S37 and T41, which is followed by its degradation through the βTrCP–ubiquitin pathway (Valenta et al., 2012; Stamos and Weis, 2013). However, in the presence of Wnt ligands, the sequestration of Dishevelled and Axin through the Frizzled–LRP5 or Frizzled–LRP6 receptor complex reduces the availability of the cytoplasmic destruction complex and results in the accumulation of cytosolic β-catenin (Mao et al., 2001; Zeng et al., 2005; Bilic et al., 2007; Li et al., 2012; Kim et al., 2013). Subsequently, β-catenin enters the nucleus and engages lymphoid enhancing factor/T-cell factor (LEF/TCF) family transcription factors to initiate transcription of target genes (Cadigan and Waterman, 2012; Valenta et al., 2012). Canonical Wnt–β-catenin signaling functions primarily by triggering the transcription of target genes, in which the formation of the β-catenin–TCF complex is considered to be a key step.

Since the identification of the first transcriptional Wnt–β-catenin target gene, *engrailed*, multiple approaches have been developed to explore Wnt targets, which have resulted in a Wnt targetome sketch containing hundreds of genes (DiNardo et al., 1988; Vlad et al., 2008). Notably, genes involved in cell proliferation are over-presented in the target list. In agreement with this, the promotion of cell proliferation is considered one of the most typical cellular functions of Wnt–β-catenin signaling (Logan and Nusse, 2004). Indeed, Wnt stimulates the G1/S transition by activating its direct targets MYC and CCND1 (cyclin D1), as well as by downregulating molecules that inhibit the cell cycle, such as CDKN2A (also known as p21) (Niehrs and Acebron, 2012). Numerous studies have also demonstrated that Wnt signaling can promote proliferation in various tissues and cell types, such as neural stem cells, endothelial cells and pancreatic β-cells (Masckauchán et al., 2005; Rulifson et al., 2007; Pei et al., 2012). In particular, Wnt signaling is required for the routine renewal cycle of intestinal and colonic tissues (Gregorieff and Clevers, 2005; Clevers, 2006). Moreover, hyper-activation of Wnt signaling resulting from APC, AXIN or β-catenin mutations triggers uncontrolled cell proliferation and eventually leads to cancer (Clevers and Nusse, 2012). Conversely, inhibition of Wnt signaling through expression of dominant-negative TCF induces G1 or G2 arrest (van de Wetering et al., 2002; Vijayakumar et al., 2011).

In addition to promoting cell proliferation, components of the Wnt pathway, such as AXIN2, β-catenin, GSK3β and APC, also participate in execution of the mitotic program. This includes spindle assembly, microtubule rearrangement and centrosome division (Niehrs and Acebron, 2012). During these processes, AXIN2, GSK3β and β-catenin localize at the centrosome while APC and AXIN2 accumulate on the spindle in order to perform their normal function (Huang et al., 2007; Hadjihannas et al., 2010; Chilov et al., 2011).

[1]MOE Key Laboratory of Protein Science, School of Life Sciences, Tsinghua University, Beijing 100084, China. [2]School of Life Sciences, Peking University, Beijing 100871, China. [3]MOE Key Laboratory of Bioorganic Phosphorus Chemistry and Chemical Biology, Tsinghua-Peking Center for Life Sciences, Department of Chemistry, Tsinghua University, Beijing 100084, China. [4]The State Key Laboratory of Biomembrane and Membrane Biotechnology, Tsinghua-Peking Center for Life Sciences, School of Life Sciences, Tsinghua University, Beijing 100084, China.
*These authors contributed equally to this work

‡Author for correspondence (wwu@mail.tsinghua.edu.cn)

Received 25 November 2013; Accepted 10 September 2014

Journal of Cell Science

Journal of Cell Science (2014) 127, 4833–4845 doi:10.1242/jcs.146977

Cell death and survival are also regulated through Wnt signaling (Pećina-Šlaus, 2010). In most reported cases, inhibition of Wnt signaling increases apoptosis, whereas activation of Wnt protects cells from agent-induced and intracellular apoptosis, although there have been a few exceptions where Wnt activation leads to cell death (Chen et al., 2001; You et al., 2002; Olmeda et al., 2003; Zimmerman et al., 2013). Many genes involved in anti-apoptotic processes, such as the IAP (inhibitor of apoptosis) family members *BIRC5* and *BIRC7* (namely survivin and livin, respectively) were also identified as Wnt targets (Zhang et al., 2001; Huang et al., 2006; Yuan et al., 2007). These data thus establish that Wnt signaling has a key role in cell survival.

Interestingly, Wnt signaling fluctuates throughout the cell cycle. For example, the level of β-catenin protein along the course of the cell cycle is not constant, but instead is elevated in S-G2 (herein, S-G2 denotes S and G2 phases, whereas G2-M denotes G2 and M phases) (Olmeda et al., 2003). Moreover, the Wnt receptor LRP6 is highly phosphorylated during mitosis by cyclin Y (also known as CCNY) and its related cyclin-dependent kinase (CDK14). Consistently, Wnt-responsive reporter expression was found to be higher in G2-M cells than that in G1 (Davidson et al., 2009). These data indicate that there are distinct Wnt signaling activities at different cell cycle stages. Paradoxically, mRNA levels of Wnt target genes, such as *AXIN2* (a negative-feedback regulator also known as conductin/axil) and *LGR5* [a co-receptor for R-spondin1 and a positive modulator of β-catenin signaling (de Lau et al., 2011; Glinka et al., 2011)], peak at the G2-M phase, whereas *MYC* mRNA accumulates in the G1-S phase (Rabbitts et al., 1985; Hadjihannas et al., 2012). In the same report, it was also shown that phosphorylated β-catenin, which should be subjected to ubiquitylation and degradation, was enriched during the S-G2 phase (Hadjihannas et al., 2012). From these results, it was concluded that Wnt–β-catenin signaling is relatively low in the G2 phase. These observations emphasize the complexity of the interplay between Wnt signaling and the cell cycle, furthering the controversy over which cell cycle phase possesses the highest level of Wnt signaling. Notably, previous studies reporting the influences of the cell cycle on Wnt signaling focused on the upstream regulation of the Wnt pathway, whereas the status of the core transcriptional activation complex, β-catenin–TCF, has not yet been deciphered in the cell cycle context. Thus, the precise dynamics of Wnt activity during the cell cycle, particularly the transcriptional regulation of Wnt targets, require further study.

To gain insight into the regulation of Wnt signaling during the cell cycle, especially the status of the core transcriptional activation complex, we developed a bimolecular fluorescence complementation (BiFC) biosensor to visualize the β-catenin–TCF interaction in living cells. With the assistance of this tool, we show that the amount of the nucleus-localized β-catenin–TCF complex increases during S-G2 and declines when cells re-enter the G1 phase. Accordingly, a subset of Wnt target genes was found to be transcriptionally regulated through the β-catenin–TCF complex during the S-G2 phase. These results could help to answer the long-standing question of why the Wnt signal is highly stimulated at this stage of the cell cycle.

RESULTS

Visualization of the β-catenin–TCF complex by using BiFC

To detect the β-catenin–TCF interaction in living cells, we designed a BiFC biosensor system using fragments derived from fluorescent protein Venus or yellow fluorescent protein (YFP) (Kerppola, 2006; Shyu et al., 2006). According to the crystal structure of the β-catenin–TCF3 complex (Graham et al., 2000), we fused either the N-terminal half of Venus (VN) or the N-terminal half of YFP (YN) to the N-terminus of TCF3, and either the C-terminal half of Venus (VC) or the C-terminal half of YFP (YC) to the C-terminus of β-catenin (supplementary material Fig. S1A). Interaction between β-catenin and TCF3 thereby enabled reconstitution of an intact bimolecular fluorescent complex (supplementary material Fig. S1A). Because aberrant activation of Wnt–β-catenin signaling might trigger apoptosis (Kim et al., 2000; Olmeda et al., 2003), the transactivation domain of β-catenin (the C-terminal 113 amino acid residues) was truncated to keep the transcriptional activity of β-catenin–TCF at a moderately low, if not null, level (supplementary material Fig. S1B). Through transient transfection, we were able to overexpress our Venus or YFP biosensor systems in HeLa cells and observed BiFC signal specifically in the nucleus (left column, Fig. 1A), where the β-catenin–TCF complex forms. The Venus system enabled the direct visualization of protein–protein interactions under physiological conditions (37℃), whereas the YFP system required that the cells were pre-incubated at a lower temperature (30℃) to stabilize BiFC signals (Kerppola, 2006).

Next, we tested the specificity of the BiFC signal system. To do this, two mutant forms of TCF3, TCF3ΔNLS and TCF3ΔN, were incorporated into the BiFC system instead of wild type. In the TCF3ΔNLS construct, the nuclear localization signal sequences had been deleted, thus it was expected to be retained in the cytosol. In TCF3ΔN, the N-terminal β-catenin binding domain had been largely eliminated, thus it was expected to be unable to bind to β-catenin. As shown in Fig. 1A, the β-catenin–TCF3ΔNLS complex localized exclusively in the cytoplasm, whereas BiFC signals derived from β-catenin–TCF3ΔN were barely detected. Moreover, consistent with their roles in β-catenin degradation and TCF binding competition (Orsulic et al., 1999), the BiFC signal derived from β-catenin and wild-type TCF3 was strongly reduced upon co-expression of either GSK3β or E-cadherin (also known as CDH1), respectively (upper panels, supplementary material Fig. S1C). Of note, GFP expression was not changed by either treatment, thus further supporting that the reduction of the BiFC signal was specific (lower panels, supplementary material Fig. S1C). Collectively, these results suggest that the nuclear BiFC signal originated specifically from β-catenin and TCF interactions.

β-catenin–TCF BiFC signals accumulate in the S and G2 phases of the cell cycle

Next, HeLa cell lines stably expressing doxycycline-repressible β-catenin–TCF BiFC were generated, in which FLAG-β-catenin-VC and Myc-VN-TCF3 constructs were simultaneously induced using the pBI bidirectional vector system (supplementary material Fig. S1D) (Baron et al., 1995). A control cell line expressing inducible Venus was generated using the same strategy. Both the FLAG–β-catenin–VC and the Myc–VN–TCF3 proteins were specifically induced upon the withdrawal of doxycycline (upper panel, supplementary material Fig. S1E). The level of induced β-catenin was comparable to that of endogenous β-catenin (lower panel, supplementary material Fig. S1E). In these cell lines, nucleus-localized BiFC signals were specifically induced by withdrawing doxycycline, but only in about 10% of cells (data not shown).

To exclude variations in integration sites and copy numbers among cells, the stable cell lines were amplified from single cells

Journal of Cell Science (2014) 127, 4833–4845 doi:10.1242/jcs.146977

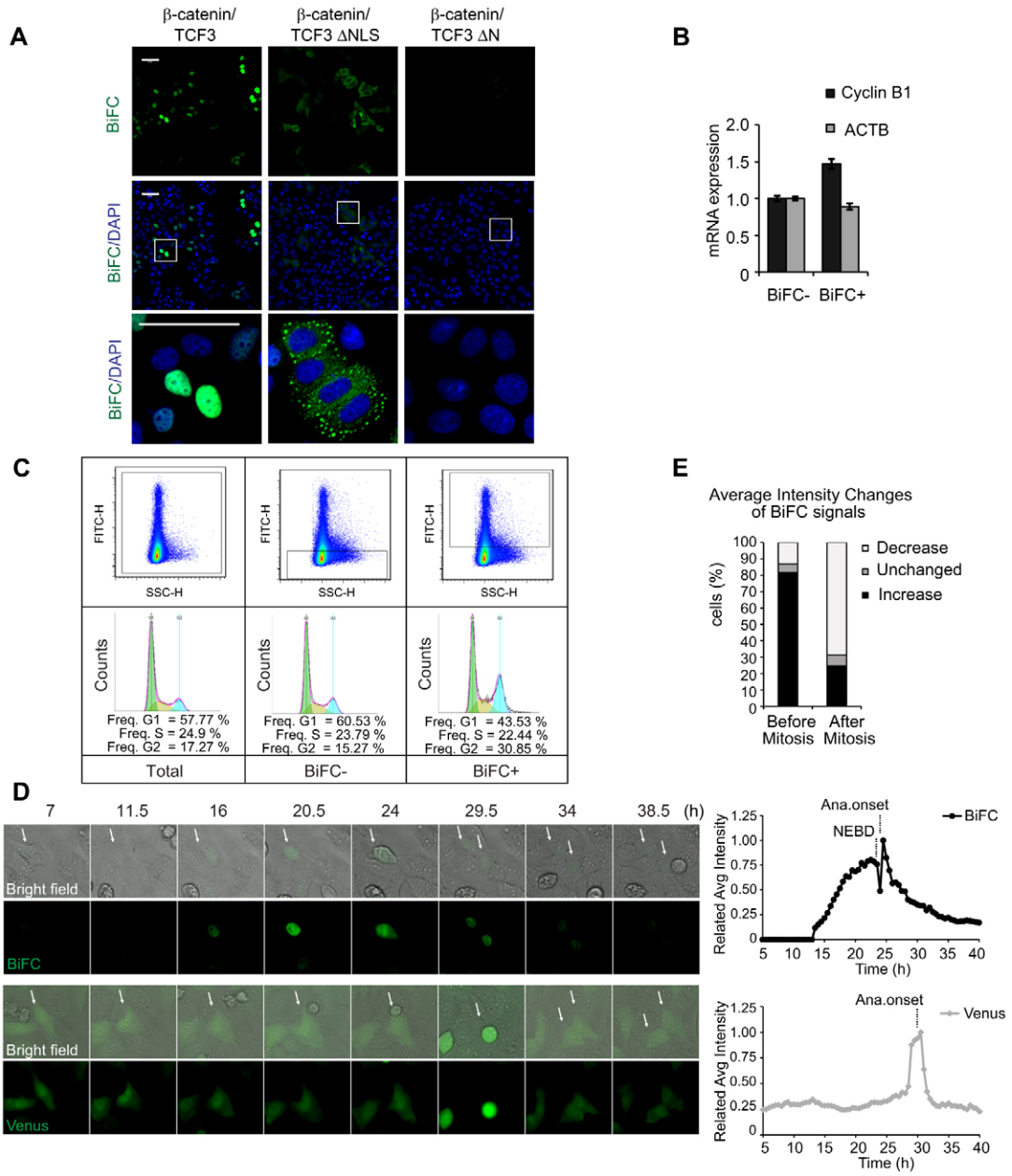

Fig. 1. β-catenin–TCF BiFC signal accumulates during the S-G2 phases. (A) HeLa cells expressing the β-catenin–TCF BiFC biosensors. β-catenin-VC (β-catenin) was co-transfected with VN-TCF3 (TCF3), VN-TCF3ΔNLS (TCF3ΔNLS) or VN-TCF3ΔN (TCF3ΔN). The third row shows the enlarged view of the corresponding boxed regions. Scale bars: 50 μm. (B) Real-time PCR analysis of BiFC-positive and -negative cells for the indicated genes. Values were normalized to *RPLP0* mRNA. *ACTB* (β-actin) was used as a control. Error bars represent s.d. (n=3). (C) Flow cytometry analysis of DNA content and GFP signal intensity in live BiFC cells that had been stained with the cell-permeable DNA dye Hoechst 33342. The DNA profiles of the total, BiFC-positive or -negative gated populations are shown. (D) Left: dynamics of the BiFC and Venus signal during cell cycle progression. Images were acquired every 30 min for a total of 40 h. Images captured by using fluorescence and phase-contrast (bright field) microscopy are shown. Right: quantification of the average fluorescence intensity of the BiFC and Venus signals during cell cycle progression. Ana. onset, the onset of anaphase; NEBD, nuclear envelope breakdown. (E) Statistics of the BiFC dynamics during the cell cycle shown in (D). Of the BiFC-positive dividing cells, 81.6% showed ascending signals before mitosis (n=38) and 68.9% showed descending trends after mitosis (n=61). Quantification of the average florescence intensity was analyzed by using IMARIS software.

and further sorted into single clones by using fluorescence-activated cell sorting (FACS) repeatedly. Surprisingly, the BiFC signal in these cells became heterogeneous after one passage and reached a stable ratio of ~10% positivity in two to three passages. This dynamic change was not observed in the Venus stable cell line expressing the intact fluorescent protein. Thus, we speculated that this heterogeneity resulted from BiFC dynamics, and that the cell cycle might be involved.

To this end, real-time PCR analysis of the β-catenin–TCF BiFC-positive and -negative cell populations revealed that the mRNA level of cyclin B1 (*CCNB1*), a G2-M phase marker (Penelova et al., 2005), was substantially higher in the β-catenin–TCF BiFC-positive fraction (Fig. 1B). Consistent with this observation, using DNA content profiling, an enrichment of G2-M cells was detected in the β-catenin–TCF BiFC-positive fraction when compared with those in either the total or negative

Journal of Cell Science (2014) 127, 4833–4845 doi:10.1242/jcs.146977

populations. Notably, both the BiFC-Venus and the BiFC-YFP β-catenin–TCF biosensor stable lines showed similar results (Fig. 1C; supplementary material Fig. S2). Therefore, we hypothesized that the β-catenin–TCF BiFC signal was enriched in G2-M cells.

To test this hypothesis, time-lapse analyses of the BiFC signals were performed. The BiFC signals were continuously monitored for 40 h by using high content screening (HCS), which allows large-scale and real-time scanning. A sharp increase of the average intensity of the BiFC signal was observed before mitosis in most BiFC-positive cells (Fig. 1D,E; supplementary material Movies 1, 2). The fluorescent signals were then released from the nucleus into the whole cell with the collapse of the nuclear envelope. During anaphase and cytokinesis, BiFC signals were evenly distributed into two daughter cells, but as cells entered into the next G1 phase, the BiFC signals gradually decreased to almost undetectable levels (Fig. 1D; supplementary material Movies 1, 2). Approximately 81.6% of the BiFC-positive dividing cells exhibited ascending signal intensities before mitosis and 68.9% exhibited descending fluorescent signals after mitosis as quantified with IMARIS software (Fig. 1E). However, a few daughter cells were observed behaving differently. In these cells, upon separation, the BiFC signal in one daughter cell declined gradually, whereas, in the other cell, the signal became even stronger. Many of these brighter cells eventually died. The phenomenon that BiFC signals increased during the S-G2 phase was also confirmed using cells released from a thymidine block regime (supplementary material Movie 3). By contrast, similar changes were not observed in the Venus stable control cell line. Indeed, the average intensity of the Venus signal remained steady during interphase and only increased when cells were rounded up for mitosis (Fig. 1D; supplementary material Movies 4, 5). As the BiFC signal originates specifically from the β-catenin–TCF complex, these results suggest that the amount of β-catenin–TCF complex fluctuates with cell cycle progression. Specifically, it accumulates in the S phase, peaks at the G2 phase and declines in the G1 phase.

The endogenous nuclear β-catenin–TCF4 complex is enriched during the S and G2 phases in colon cancer cells

Based on the observation that β-catenin–TCF-generated BiFC signals are dynamic during the cell cycle, we further hypothesized that there was an oscillation of the interaction between endogenous β-catenin and TCF during cell cycle. Colon cancer HCT116 cells were chosen to test our hypothesis as they bear a wild-type APC gene but have a deletion of residue S45 in one allele of β-catenin (Li et al., 2012). Therefore, they exhibit constitutive Wnt–β-catenin signaling and do not require ligand stimulation. This cell line has also been confirmed to have an intact Wnt signaling cascade upstream of β-catenin (Li et al., 2012). TCF4 was analyzed because it is the most predominantly expressed and functional member of the TCF genes in the colonic and intestinal epithelium and is important for the proliferation of colon cancer cells (Korinek et al., 1997; Batlle et al., 2002; Najdi et al., 2009).

To test endogenous protein–protein interactions at different cell cycle stages, we first used a thymidine block to synchronize cells at the early S phase, and then released them to progress through the full cell cycle. Cells were harvested at different timepoints and the degree of synchronization was analyzed by using flow cytometry (Fig. 2A). Cells were then separated into two fractions: a nuclear fraction and a detergent-soluble cytosol-membrane fraction. Consistent with a previous report (Olmeda et al., 2003), western blot experiments indicated that the amount of nucleus-localized β-catenin increased during S-G2, but quickly dropped to basal levels once the cells returned to G1 (Fig. 2B). Meanwhile, the amount of β-catenin in the cytosol-membrane fraction stayed constant throughout the cell cycle. TCF4, conversely, was exclusively localized in the nucleus; the level of the protein slightly increased when cells were released from the early S phase and thereafter remained steady (Fig. 2B).

Next, co-immunoprecipitation experiments were used to detect interactions between β-catenin and TCF4 in the nuclear fraction during the cell cycle. Substantial enrichment of the β-catenin–TCF4 complex was detected during the S-G2 phase, whereas a decline was observed as cells entered the next G1 phase (Fig. 2C). Therefore, consistent with the dynamics of the BiFC signal, the amount of endogenous β-catenin–TCF complex in HCT116 cells increases during the S phase, peaks at G2 and decreases in the G1 phase of the cell cycle.

Transcriptional targets of the β-catenin–TCF complex during the S and G2 phases of the cell cycle

Because β-catenin interacts with the LEF/TCF family of transcription factors in the nucleus to initiate target gene expression, the accumulation of the β-catenin–TCF complex in the nucleus during the S-G2 phase might imply that Wnt target genes are transcribed during this time window. Therefore, we next investigated the expression of Wnt target genes in S-G2 phase cells.

First, the expression levels of 515 genes that are reported to be responsive to Wnt stimulation were profiled in HCT116 cells through microarray experiments. Of these, 342 were confirmed to be expressed (supplementary material Tables S1, S2). These genes were analyzed for gene ontology (GO) term classification using the DAVID program and were found to be mainly linked to six biological processes (Fig. 3A; supplementary material Tables S3–S5). Consistent with typical functions of Wnt signaling in colon cancer cells, genes related to cell proliferation were substantially enriched in this pool. Genes related to cell death and cell cycle also exhibited enrichment greater than 10% (Fig. 3A) and were selected for further analysis owing to their strong affiliation with the S-G2 phase. Consequently, the list was simplified to 42 genes of which the promoters contained consensus LEF/TCF binding sites and their occupancy by β-catenin or TCF/LEF was experimentally verified (supplementary material Table S6).

We then set out to investigate whether the transcription of these genes was controlled by the β-catenin–TCF complex in the S-G2 phase. To do this, specific inhibitors were used to block the formation of the complex during these phases. The inhibitors needed to be supplied and effective in a relatively short time period in HCT116 cells, starting at the G1/S transition and finishing at the G2/M transition, ~8 h in total. Dominant-negative TCF4 is a well-characterized inhibitor of β-catenin binding to DNA-associated TCF4 (van de Wetering et al., 2002); however, it is impossible for the Tet-On/Tet-Off inducible system to produce enough protein in such a short time window. Instead, we employed other types of inhibitors, including the small molecular inhibitor iCRT and the stapled peptide inhibitor aStAx-35R (herein referred to as aStAx), both of which are reported to disrupt the β-catenin–TCF4 association (Gonsalves et al., 2011; Grossmann et al., 2012). For inhibitor assays, synchronized HCT116 cells were released and treated simultaneously with

Journal of Cell Science (2014) 127, 4833–4845 doi:10.1242/jcs.146977

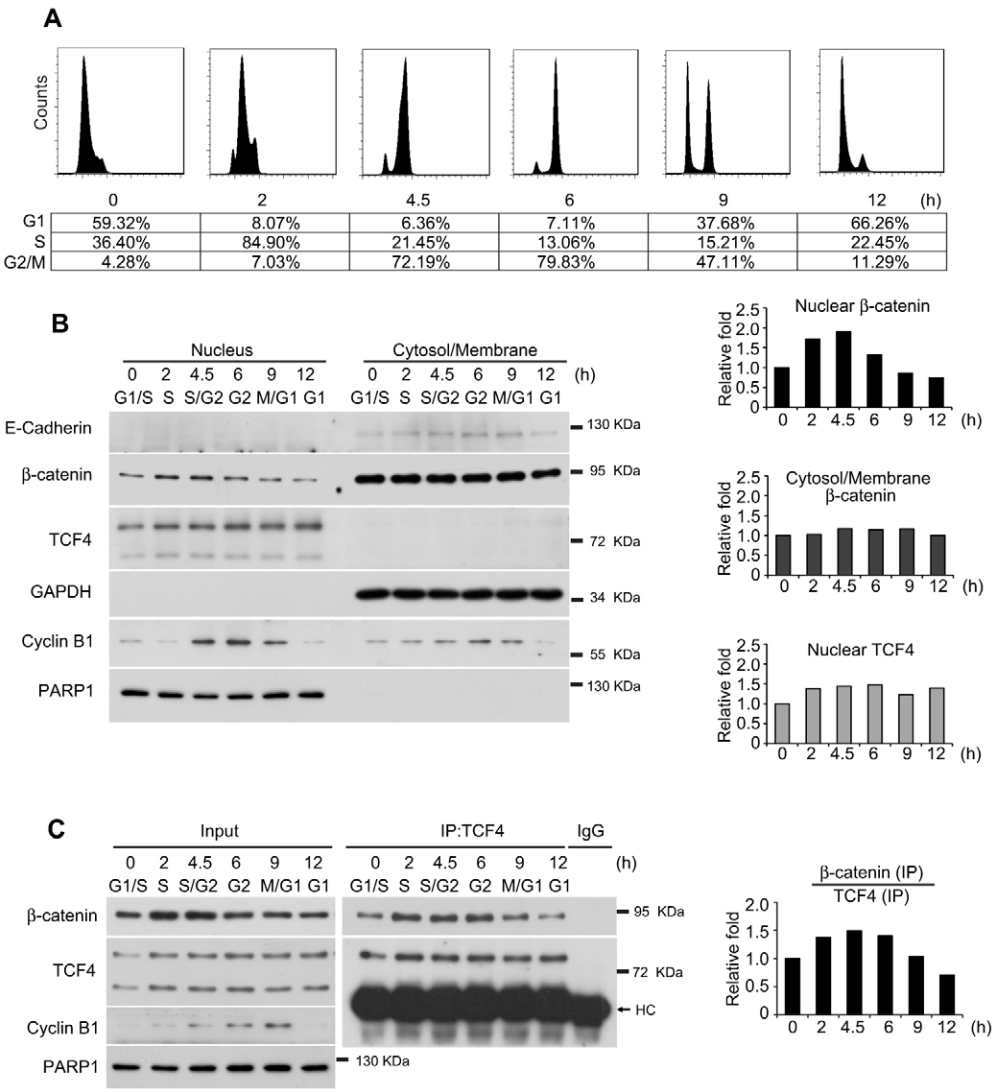

Fig. 2. The endogenous nuclear β-catenin–TCF4 complex is enriched during the S-G2 phases. (A) Flow cytometry analysis of HCT116 cells that had been synchronized by using thymidine block and then released at the indicated timepoints. The stage of the cell cycle was analyzed by using propidium iodide (PI) staining and flow cytometry. (B) Left, western blot analysis of cell lysates from samples harvested in A. The nuclear and cytosol-membrane fractions were separated. Right, nuclear β-catenin and TCF4, and cytosol-membrane β-catenin levels were normalized to those of PARP1 or GAPDH, respectively. Quantification of the results from the six timepoints were further normalized to that of time 0 h. Graphs shown in B and C are quantification results from corresponding western blot images. Band intensities were quantified by using ImageJ software. (C) Left, western blot analysis of nuclear extracts (input) or immunoprecipitates (IP) with the TCF4 antibody or a mouse IgG as control from cell samples harvested in A. Right, the levels of immunoprecipitated β-catenin were normalized to that of the corresponding TCF4 immunoprecipitation. Quantification of the results from all six timepoints were further normalized to that of time 0 h.

vehicle, iCRT or aStAx for 8 h such that the interaction of β-catenin and TCF4 was inhibited exactly during the S-G2 phase, as shown in Fig. 3B. Importantly, upon treatment with iCRT, the mRNA expression levels of 23 of the 42 genes were significantly downregulated ($P<0.05$) (Fig. 3C; supplementary material Fig. S3A). The downregulation of 10 of these 23 genes was further confirmed upon treatment with aStAx (supplementary material Fig. S3B). The slight inconsistency between the two inhibitors might reflect their different capacities to inhibit Wnt-mediated transcription as measured by the TOP-Flash reporter and cell proliferation assays. Indeed, aStAx was a much weaker inhibitor than iCRT in our system (supplementary material Fig. S3C–E). Collectively, our data suggest that the transcription of a subset of Wnt target genes during the S-G2 phase is, at least, partially mediated by the β-catenin–TCF complex.

To confirm that these genes were indeed transcribed in S-G2 cells, we also performed nascent RNA capture assays to detect newly synthesized transcripts during this phase. Briefly, HCT116 cells were synchronized and then released into iCRT- or vehicle-containing medium for 6 h before harvest. The labeling reagent 5-ethynyl uridine (EU) was introduced at the 4-h timepoint to label newly synthesized mRNAs. In the presence of iCRT, statistically significant decreases in nascent transcript levels were observed for 21 of the 23 genes when compared with those in the vehicle control (Fig. 3D), indicating that the transcription of these 21 genes at the S-G2 phase is Wnt dependent. To further confirm

Journal of Cell Science (2014) 127, 4833–4845 doi:10.1242/jcs.146977

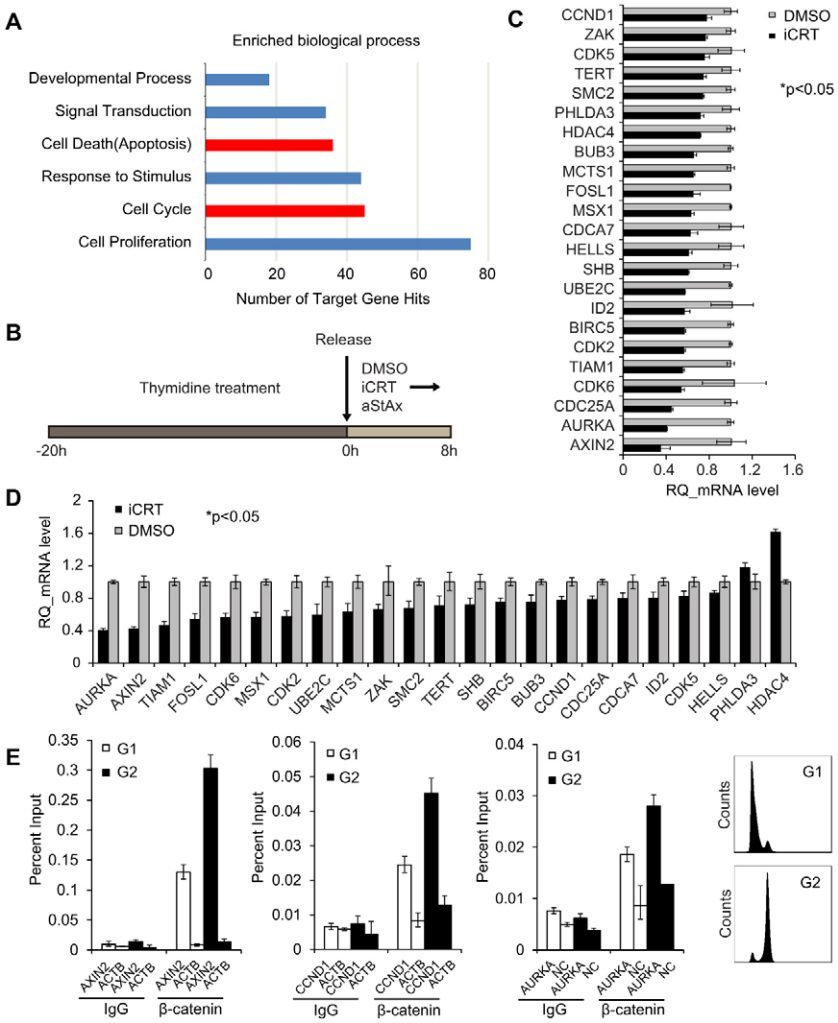

Fig. 3. Identification of the transcription targets of the β-catenin–TCF complex during the S-G2 phases. (A) Major categories of biological processes that are enriched in Wnt target genes in HCT116 cells. Significantly enriched processes were selected by using the raw *P*-value and false discovery rate method (FDR) corrected *P*-value at thresholds of 0.05 and 0.1, respectively. The items highlighted in red were selected for further verification. (B) The experimental scheme of Wnt target verification during the S-G2 phase. After a 20-h thymidine block, HCT116 cells were released into medium containing DMSO, iCRT or aStAx for 8 h (precisely in S-G2) and then harvested for the assay shown in C. (C) Downregulation of Wnt target genes during the S-G2 phase upon treatment with iCRT. The expression levels of genes involved in cell death and cell cycle progression were determined by using real-time PCR. Values were normalized to *RPLP0* mRNA. The results are the average of triplicate data; the s.d. and *P*-values were calculated by using a two-tailed Student's *t*-test. Genes shown here are those that could be repeatedly and significantly ($P<0.05$) downregulated by using iCRT in three independent assays; the full dataset of 42 genes is shown in supplementary material Fig. S3A. RQ_mRNA, relative quantification of mRNA level. (D) Inhibition of nascent mRNA synthesis of Wnt target genes upon treatment with iCRT during the S-G2 phase. iCRT was added as shown in panel B. EU was added at the 4 h timepoint. Labeling was terminated at the 6-h timepoint, and cells were harvested for total RNA isolation. On-bead cDNAs were prepared and examined by using quantitative PCR. The results are the average of triplicate data; the s.d. and *P*-values were calculated by using a two-tailed Student's *t*-test. (E) Chromatin immunoprecipitation assays in G2- or G1-enriched HCT116 cell populations (5 h or 12.5 h after release from the thymidine block). The promoter regions of *AXIN2*, *CCND1* and *AURKA* (graphs from left to right) were tested and the promoter of *ACTB* (β-actin) was used as a control. All graphs show the means±s.d. ($n=3$). The cell cycle profiling of G1 or G2 phase HCT116 cells is shown in the right panel.

that the β-catenin–TCF complex indeed triggers gene transcription in S-G2, chromatin immunoprecipitation (ChIP) assays were performed using populations enriched for cells in G1 or G2. Interestingly, more β-catenin was detected bound to the promoter regions of several Wnt target genes, such as *AXIN2*, *AURKA* and *CCND1*, in G2 phase cells when compared with those from G1, as analyzed by using real-time PCR with ChIP-enriched DNA fragments Fig. 3E). By contrast, the amount of bound TCF4 remained constant at the two phases (supplementary material Fig. S3F). These results are consistent with previous reports that TCF binds to target genes constantly, whereas β-catenin binding determines gene transcription (Cadigan and Waterman, 2012). Taken together, these results strongly suggest that the β-catenin–TCF complex triggers the expression of a subset of Wnt target genes at the S-G2 phase during cell cycle progression.

β-catenin–TCF-mediated target gene expression ensures G2/M progression

We observed that some genes required for G2/M progression, such as *CDC25A*, *AURKA* and *SMC2*, were downregulated upon inhibition of Wnt. This suggests that Wnt signaling is essential for cell cycle progression through the G2-M phase. To test this hypothesis, HCT116 cells were released from a G1/S block into

Journal of Cell Science (2014) 127, 4833–4845 doi:10.1242/jcs.146977

fresh medium or medium supplemented with iCRT, and cell cycle progression was monitored for the following 24 h. The vast majority of control cells transited into G2 phase after 4 h, exited mitosis and returned to the next G1 phase at the 10-h timepoint and then entered S phase after 13.5 h (left, Fig. 4A). Accordingly, the levels of phosphorylated histone H3, a specific mitotic marker, and CCNB1, peaked as the cells entered mitosis and fell when the process was completed (left, Fig. 4B). The phosphorylation level of CDK1 at residue Tyr15, which represents the inactivation of CDK1 (Norbury et al., 1991), decreased after 8 h, during the G2/M transition, without affecting the abundance of CDK1 (left, Fig. 4B). However, cells that were released into iCRT-containing medium progressed through S phase with a slight delay and transited into G2 phase after 6 h.

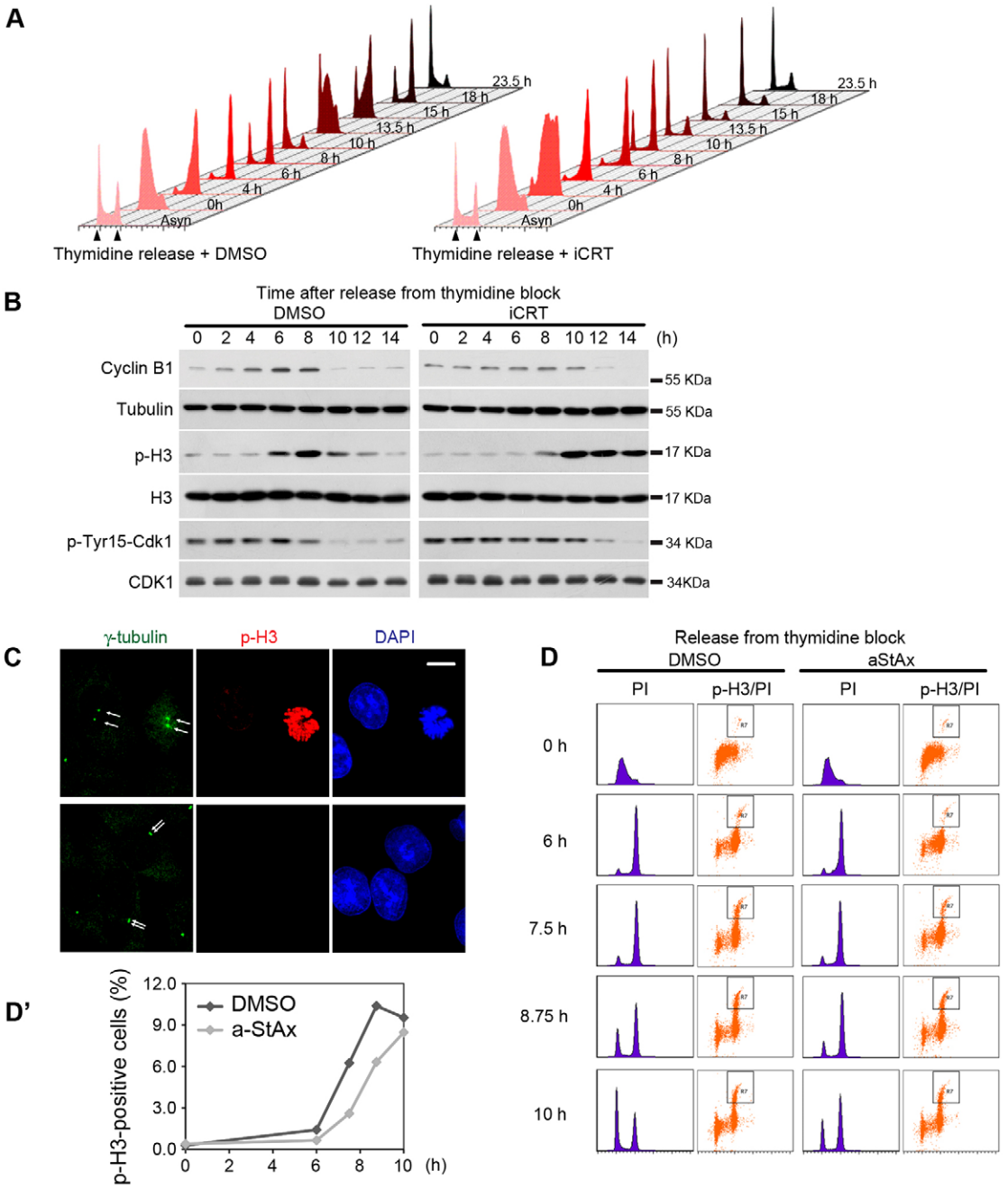

Fig. 4. β-catenin–TCF-mediated target gene expression ensures G2/M progression. (A) Delay of G2/M progression by using iCRT. Synchronized HCT116 cells were released into medium containing either DMSO (control) or 50 μM iCRT. Cells were harvested at the indicated timepoints, and their cellular DNA content was determined by using PI staining and flow cytometry. Asyn: asynchronous cells. (B) Western blot analysis of cell extracts from samples shown in A using the indicated antibodies. (C) HCT116 cells 7.5 h after release, as described in A, were stained with DAPI (blue) and for phosphorylated histone 3 (p-H3, residue S10, red) or γ-tubulin (centrosome, green) after treatment with DMSO or iCRT. Scale bar: 10 μm. (D) Delay of G2/M progression after treatment with aStAx. Synchronized HCT116 cells were treated with DMSO or aStAx following release. The mitotic index was assessed by using p-H3 and PI staining using FACS at the indicated timepoints. (E) Percentage of p-H3-positive cells (boxed population in D) after DMSO or aStAx treatment at indicated timepoints.

Journal of Cell Science

Journal of Cell Science (2014) 127, 4833–4845 doi:10.1242/jcs.146977

Division proceeded after 10 h and re-entry into the next G1 phase happened after just 13.5 h of incubation. The cells were then mostly arrested in the G1 phase until 23.5 h (right, Fig. 4A). Consistent with the DNA content changes, a lag in histone 3 phosphorylation and a weakened accumulation of CCNB1 during the G2 phase were observed. Moreover, CDK1 phosphorylation only started to decrease after 12 h in iCRT-treated cells (right, Fig. 4B).

To more pertinently verify the effects of iCRT on G1 and G2 cells, they were treated at either the S-G2 phase or after cells had entered the next G1 phase. As shown in supplementary material Fig. S4A, when iCRT was added to the released cells immediately after the thymidine block and then removed 8 h later, a delay in G2/M progression was observed (compare 10-h timepoints in supplementary material Fig. S4A1 and Fig. S4A3); however, many cells re-entered the next S and M phases after iCRT was removed (compare 20-h timepoints in supplementary material Fig. S4A3 and Fig. S4A2). When iCRT was added only 9 h after the release (to coincide with S-G2 phase entry), the entry of cells into S phase was considerably delayed (compare 14- to 18-h timepoints in supplementary material Fig. S4A1 and Fig. S4A4). These results suggest that (1) treatment with iCRT did not cause any permanent damage to the cell cycle machinery in S-G2 cells, (2) the inhibition of Wnt in S-G2 phase cells induced a delay of the G2/M transition, (3) the inhibition of Wnt in G1 phase cells induced a delay of the G1/S transition and (4) the G1 arrest observed in supplementary material Fig. S4A2 required inhibition of Wnt at both the G1 and G2 phases.

Further studies focused on monitoring how iCRT-treated cells entered and proceeded through mitosis. At 7.5 h, delayed centrosome separation was observed together with later entry into mitosis (Fig. 4C). Unlike control cells that entered mitosis simultaneously, iCRT-treated cells exhibited a much broader time window of mitosis entry, starting anywhere from the 8- to 14-h timepoint (supplementary material Fig. S4B). The amount of phosphorylated histone 3 remained at a high level during this period (right, supplementary material Fig. 4B). Notably, despite the delayed entry, the crucial mitotic processes, including DNA condensation, chromosome alignment and segregation, and cytokinesis proceeded successfully (supplementary material Fig. S4C). Thus, these results suggest that treatment with iCRT delays the G2/M transition but does not affect mitosis. Similarly, treatment with aStAx also induced a delay of G2/M progression concomitant with a lag in the accumulation of phosphorylated histone 3, as well as delayed G1 entry (Fig. 4D).

Taken together, these observations suggest that the disruption of the β-catenin–TCF complex in HCT116 cells results in a considerable delay of the G2/M transition, accompanied by a lag in the accumulation of CCNB1, histone 3 phosphorylation, activation of Cdk1 and delayed centrosome separation. These results indicate that β-catenin–TCF-mediated transcription is essential for G2/M progression in Wnt-dependent cancer cells.

β-catenin–TCF complex-mediated target gene expression ensures cell survival during S and G2-M phases

One important function of Wnt–β-catenin signaling in cancer cells is to protect against apoptosis (Pećina-Šlaus, 2010). We observed that the transcription of some anti-apoptotic genes was controlled by the β-catenin–TCF4 complex during the S-G2 phase, thus we hypothesized that in addition to cell cycle progression, another function of β-catenin–TCF signaling during the S-G2 phase is to maintain inhibition of apoptosis.

To test this, caspase-3/7 activity, an indicator of cell apoptosis, was monitored in HCT116 cells following exposure to iCRT and was found to be enhanced in a dose-dependent manner (supplementary material Fig. S4D). To further explore the relationship between apoptosis and β-catenin–TCF, doxorubicin (DOX, a typical chemotherapy drug that acts through the DNA damage process) and Purvalanol A (NG 60, a potential chemotherapy drug that functions through CDK1 inhibition) (Goga et al., 2007) were chosen to further induce apoptosis in HCT116 cells, and the effects in combination with iCRT were examined. Under these settings, caspase-3 and caspase-7 activity and apoptosis-related PARP1 cleavage were modestly increased by treatment with DOX or NG 60 alone, addition of iCRT greatly enhanced the apoptotic profile (supplementary material Fig. S4E–H). These results therefore confirm that, similar to other Wnt signaling inhibitors, iCRT sensitized HCT116 cells to apoptosis induced by treatment with either DOX or NG60 at low concentrations.

Next, we addressed whether inhibition of the β-catenin–TCF complex could enhance apoptosis in S-G2 cells (Fig. 5A). Compared with asynchronous cells, incubation of synchronized cells during the S-G2 phase with iCRT resulted in stronger caspase-3 and caspase-7 activation (Fig. 5B). This observation suggests that the cells at the S-G2 phase were highly sensitive to inhibition of Wnt. Moreover, iCRT-treated S-G2 phase HCT116 cells were more sensitive to apoptosis induced by DOX or NG 60, as indicated by increased caspase-3 and caspase-7 activity and enhanced PARP1 cleavage (Fig. 5A,C-F).

It has been shown that Wnt–β-catenin signaling suppresses apoptosis by inhibiting cytochrome *c* release from the mitochondria (Chen et al., 2001). Because cytochrome *c* release is a more upstream and specific event during the apoptotic process, we wondered whether it could be affected by iCRT in S-G2 cells. As shown in Fig. 5G, synchronized S-G2 cells were treated with either DMSO or iCRT in combination with either DOX or NG 60, then, cytochrome *c* distribution was determined by using immunofluorescence staining. In control (DMSO-treated) cells, only punctate staining of cytochrome *c* was observed, indicative of mitochondrial localization. However, in iCRT-treated cells, diffuse staining was observed, indicating the release of cytochrome *c* from the mitochondria into the cytosol. Furthermore, iCRT substantially enhanced either DOX- or NG-60-induced cytochrome *c* release (Fig. 5G,H).

These data are therefore consistent with the analysis of target gene expression shown earlier, as anti-apoptotic genes such as *ID2*, *BIRC5*, *HELLS*, *MCTS1*, *TERT* and *SMC2* were all significantly downregulated upon the disruption of the β-catenin–TCF4 complex (Fig. 3C,D). Taken together, these results indicate that Wnt–β-catenin signaling promotes cell survival during the S-G2 phase, also probably in the following mitosis, and thereby contributes to Wnt-dependent cancer cell resistance to chemotherapeutic drugs (Chikazawa et al., 2010; Abdullah and Chow, 2013) through the transcriptional activation of genes that antagonize cell death.

DISCUSSION

Using BiFC technology and co-immunoprecipitation of endogenous proteins, we discovered that the β-catenin–TCF complex accumulates during the S-G2 phases and declines in the G1 phase of the cell cycle. As the transcriptional executor of Wnt signaling, the β-catenin–TCF complex might regulate the expression of target genes, either all of them or just a subset, in

Journal of Cell Science (2014) 127, 4833–4845 doi:10.1242/jcs.146977

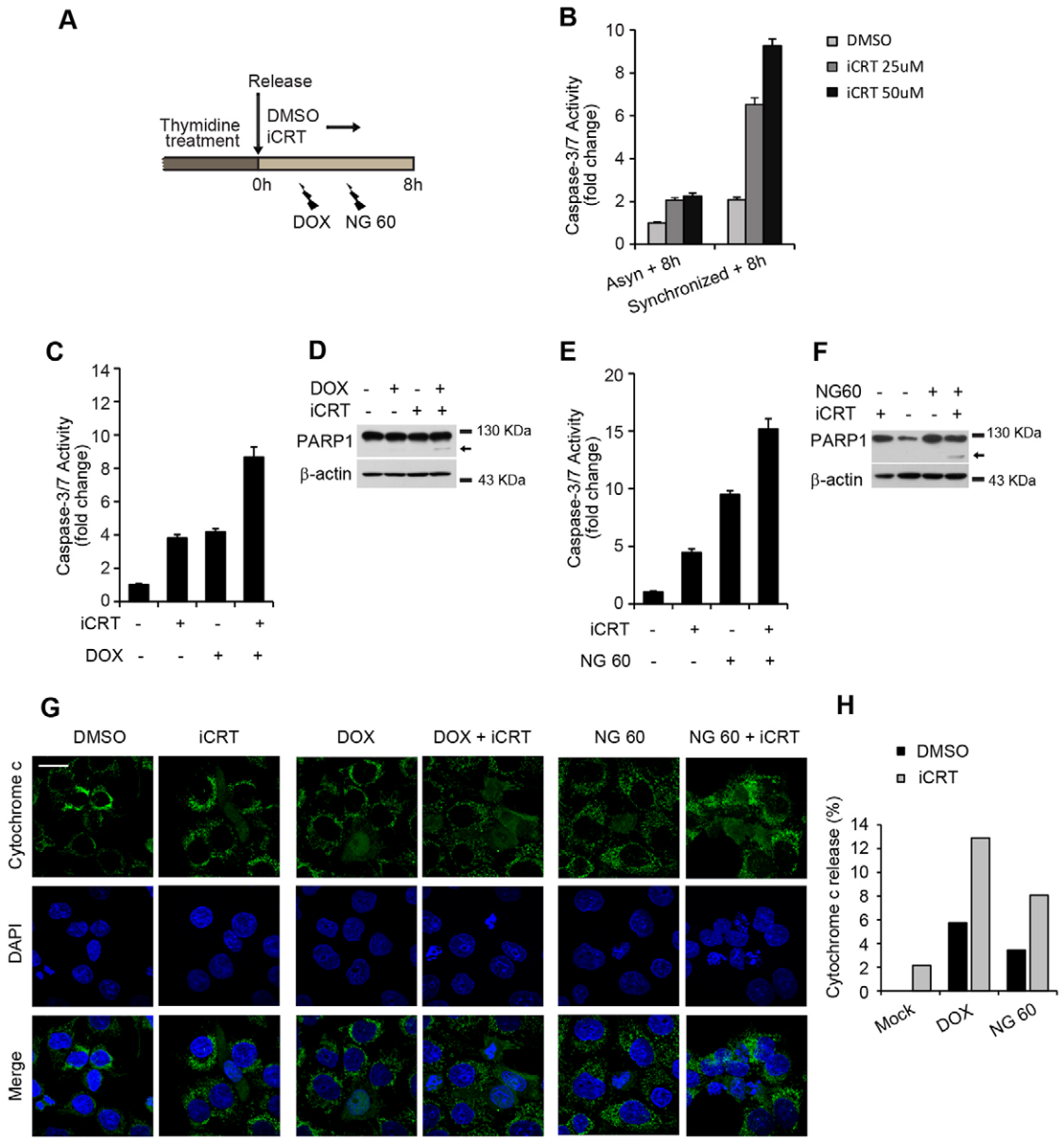

Fig. 5. β-catenin–TCF-mediated target gene expression ensures cell survival during S and G2-M phases. (A) Schematic representation of the experiments shown in B–F. Thymidine-synchronized HCT116 cells were released and treated with DMSO or iCRT in combination with DOX or NG 60 for 8 h, and then caspase-3 and caspase-7 (caspase-3/7) activity and PARP1 cleavage were determined. (B) S-G2 phase cells were more sensitive to inhibition of Wnt. Treatment with iCRT induced a stronger intrinsic-apoptosis response in synchronized S-G2 cells in comparison with asynchronous cells. Caspase-3 and caspase-7 activity was determined, and the results are the average of triplicates. Asyn: asynchronous cells. (C–F) iCRT (50 μM) sensitized S-G2 cells to apoptosis that was triggered by using doxorubicin (DOX, 1 μM) or NG 60 (5 μM). Synchronized cells were treated during the S-G2 phase, as indicated. Apoptosis was detected by using caspase-3/7 activity and PARP1 cleavage. In C and E, the results are the average of triplicates. In D and F, arrows indicate cleaved PARP1. (G) Thymidine-synchronized HCT116 cells were released into medium containing DMSO (for 8 h), iCRT (for 10 h), DOX (for 12 h), DOX + iCRT (for 12 h), NG 60 (for 12 h) or NG 60 + iCRT (for 12 h) as indicated. The cells were then fixed and stained with DAPI (blue) and an antibody against cytochrome *c* antibody (green). To ensure cells were treated during their S-G2 phases and harvested at G2 phase, different time periods were applied. Scale bar: 20 μm. (H) Quantification of cells exhibiting diffusing cytochrome *c* staining in G.

S-G2 cells. Indeed, by transiently blocking the formation of this complex with small molecule inhibitors during the S-G2 period, we observed downregulation of a group of Wnt target genes. Moreover, newly synthesized mRNAs of these genes were detected at the S-G2 stages, and their levels were reduced upon inhibition of the β-catenin–TCF complex. Finally, we showed that β-catenin and TCF indeed bound to the promoter regions of target genes at G2 phase. At the cellular level, transient inhibition of the β-catenin–TCF complex disturbed both cell survival and G2/M progression. Our results thus provide the first characterization of Wnt-signaling-regulated target gene transcription in S-G2 phase cells. They also potentiate the future dissection of mechanisms involving cell-cycle-mediated regulation of Wnt signaling.

Journal of Cell Science (2014) 127, 4833–4845 doi:10.1242/jcs.146977

G1 versus G2 Wnt signaling

Whether Wnt signaling reaches a peak in the G1 or G2-M phase has been controversial. In 1999, the cytoplasmic level of β-catenin protein was found to increase from the G1 to the S phase, and it was suggested that Wnt–β-catenin signaling might function during the G1/S transition (Orford et al., 1999). CDC20-mediated degradation of the Wnt inhibitor AXIN2 during G1-S has also been observed, further supporting a possible peak of Wnt during this time window (Hadjihannas et al., 2012). However, the level of soluble β-catenin, which is not associated with the cytoskeleton and plasma membrane, in synchronized cells is found at the maximal level in G2-M cells (Olmeda et al., 2003). Furthermore, G2-M-specific cyclin Y and CDK14 imposes priming phosphorylation on the Wnt receptor LRP6, again suggesting that Wnt signaling peaks at G2-M (Davidson et al., 2009). The discrepancy concerning the expression levels of Wnt target genes during different cell cycle stages has further added complexity to this issue, for example, *MYC* is found to be elevated at G1 whereas *LGR5* and *AXIN2* are upregulated at G2 (Hadjihannas et al., 2012). Here, we directly focused on the final executor of canonical Wnt signaling, the nuclear β-catenin–TCF complex, and observed its enrichment in S-G2 cells. We further confirmed that Wnt target genes were transcribed in this cell cycle phase. Our results thus support the conclusion that Wnt–β-catenin signaling is highly active in G2 phase cells. Although these findings were obtained from a cell culture system, our conclusion is strongly supported by the previously reported observation that hyper-activation of Wnt–β-catenin signaling occurs in G2-arrested cells in the crypt region of mouse intestine (Lee et al., 2009).

In HeLa cells, in which we established the BiFC system, Wnt signaling is relatively low, whereas in colon cancer HCT116 cells, in which we verified the amount of endogenous β-catenin–TCF complex, Wnt signaling is over-activated, largely owing to the accumulation of mutant β-catenin proteins. In either case, Wnt ligand was not significantly involved, if at all. Moreover, hyper-activation of LRP6 phosphorylation through G2-M kinases seems to happen only in the G2-M phase, whereas the accumulation of the β-catenin–TCF complex begins earlier. Therefore, it seems that cells have an intrinsic mechanism to control the oscillation of basal β-catenin–TCF complex levels, which is still maintained when the overall level of β-catenin is elevated in colon cancer cells. The capacity that cells have to produce or allow a higher level of β-catenin–TCF complex during the S-G2 phase might therefore provide a basis for the ligand stimulation during the G2-M phase, as observed previously by Davidson and colleagues (Davidson et al., 2009). The accumulation of cytosolic β-catenin during the S-G2 phase might thus result in the elevation of β-catenin that is phosphorylated at residues S33, S37 and T41 in SW480 colon cancer cells (Hadjihannas et al., 2012). We also noted that the oscillation pattern of the level of nuclear β-catenin and that of the β-catenin–TCF complex were similar, although not identical (Fig. 2B,C). This is likely to be because the two phenomena are inter-dependent, as TCF binding could protect β-catenin from being shuttled into the cytosol and subsequently degraded (Lee et al., 2001). In other words, increased TCF binding could lead to the accumulation of β-catenin itself.

The mechanism leading to the oscillation of the β-catenin–TCF complex throughout the cell cycle is not clear, but it seems more probable that the β-catenin–TCF complex per se possesses regulatory hot spots. Indeed, post-translational modifications of both β-catenin and TCF have been repeatedly reported to influence their localization, complex formation and activation of target genes (Cadigan and Waterman, 2012; Valenta et al., 2012; Gao et al., 2014).

S-G2-specific functions of the Wnt–β-catenin signaling

A role of Wnt–β-catenin signaling in triggering the G1/S transition and cell proliferation has been elaborated and believed to occur largely through the induction of *MYC* and *CCND1* (Schweinfest et al., 1988; Resnitzky et al., 1994). Here, we show that the β-catenin–TCF transcription complex is enriched in G2 cells, thus pinpointing the existence of Wnt target gene transcription in this cell cycle phase. We further confirm that in colon cancer cells, in which Wnt signaling is highly active and important for cell cycle progression, inhibition of β-catenin–TCF complex formation reduces the expression of key genes that are responsible for the G2/M transition, causing cell cycle delay. Among the genes that were significantly downregulated were *AXIN2*, *CDC25A* and *AURKA*, all of which are important in the G2-M phase of the cell cycle. *AXIN2*, the most dramatically downregulated target gene, is required for centrosomal cohesion (Hadjihannas et al., 2010). *CDC25A* is essential for mitotic entry. Indeed, G2 delay is caused by small interfering RNA against *CDC25A*, and cells that have been microinjected with small interfering RNA against *CDC25A* exhibit delayed commencement of centrosome separation (Lindqvist et al., 2005). *AURKA* is required for centrosome maturation and accurate chromosome segregation, whereas its depletion delays mitotic entry (Liu and Ruderman, 2006). Taken together, our results suggest that β-catenin–TCF-triggered expression of target genes in the S-G2 phase contributes to Wnt-mediated cell cycle progression. Consistently, the Wnt signal promotes cell survival by overcoming G2/M arrest that is induced by prolonged microtubule disruption (Aoki et al., 2007). Also, inhibition of Wnt causes G2 arrest in osteosarcoma (Leow et al., 2010) and colorectal tumor cells (Sekiya et al., 2002; Shan et al., 2009).

Promoting cell survival is another profound function of Wnt signaling (Khan and Bendall, 2006; Lento et al., 2013). Here, we show that the cells in the S-G2 phase are more sensitive to apoptosis that is induced by inhibition of Wnt than those which are unsynchronized. This was concomitant with the downregulation of genes known to be related to cell survival, such as *ID2*, *BIRC5*, *HELLS*, *TIAM1*, *MCTS1*, *TERT* and *SMC2*. TIAM1, a guanine nucleotide exchange factor, has been shown to enhance resistance to anoikis (apoptosis due to detachment) in SW480 colon cancer cells and thereby promotes cell survival and tumor metastasis (Minard et al., 2006). BIRC5 (commonly known as survivin) is a typical anti-apoptotic factor in colon tissues, and its increased expression positively correlates with tumor survival (Vaziri et al., 2005; Hernandez et al., 2011). Given that cells require more protection against DNA-damage-induced apoptosis during the S-G2 phase (Bartek et al., 2004; Huang et al., 2005), promoting the expression of anti-apoptotic genes during this period might present a fundamental function of Wnt–β-catenin signaling.

Undoubtedly, Wnt signaling has many more cellular functions – for example, control of cell differentiation, cell migration, cancer metastasis and even energy homeostasis (Rao and Kühl, 2010; Elghazi et al., 2012; Ouyang et al., 2013). How these activities are coordinated with cell cycle progression is largely unknown. A comprehensive understanding of β-catenin–TCF-regulated target

gene expression throughout the cell cycle will be extremely important in the exploration of these relationships, and ChIP-sequencing analysis in synchronized cells could be informative.

Understanding the functions of cellular signals at a particular cell cycle stage is emerging as a field of considerable research interest. For example, a recent report has demonstrated that complex regulation of the cell cycle impacts on TGFβ–Smad signaling, which in turn influences stem cell differentiation (Dalton, 2013; Pauklin and Vallier, 2013). That study and our current work highlight restrictive activities of cell cycle status to the extracellular signals imposed on the cells. It seems that the cellular function of a particular cell signal is not only dependent on the cell type but also the stage of the cell cycle.

MATERIALS AND METHODS

Cell culture, transfection and luciferase reporter assay

The colorectal cancer cell line HCT116 was grown in McCoy's 5A medium. HEK293T and HeLa-tTA cells were grown in Dulbecco's modified Eagle's medium. Transfections and Luciferase reporter assays were performed as described previously (Zhu et al., 2012).

Antibodies and reagents

Primary antibodies against β-tubulin (KM9003) and GAPDH (KM9002) were purchased from Sungene. The antibody against β-actin (M20010) was from AbMart. The FLAG M2 antibody (F3165) and the antibody against γ-tubulin (T3559) were from Sigma. The antibodies against Myc (sc-40), cyclin B1 (sc-245), CDK1 (sc-54) and PARP1 (sc-8007) were from Santa Cruz Biotechnology. The antibody against β-catenin (610154) was from BD Biosciences. The antibodies against TCF4 (2953), histone 3 (9715), lamin A/C (4777), γ-H2AX (2577), cleaved caspase-3 (9664), phosphorylated CDK1 (9111) were from Cell Signaling Technology. The antibody against phosphorylated histone 3 (at residue S10) (06-570) was from Upstate. The antibody against cytochrome *c* (AC909) was from Beyotime.

Small molecules iCRT14 (SML0203), doxorubicin hydrochloride (D1515, Sigma) and Purvalanol A (NG 60, P4484) were purchased from Sigma. The stapled peptide aStAx-35R was synthesized as described previously (Grossmann et al., 2012).

BiFC

BiFC assays were constructed as described previously (Kerppola, 2006). Venus fluorescence protein was selected as the reporter for complementation. Human β-catenin (amino acids 1–667) and *Xenopus* TCF3 (full length) were fused, respectively, with the carboxyl- (VC, amino acids 155–239) and amino- (VN, amino acid 1–173) terminal of Venus and then subcloned into the multiple cloning site of pBI bidirectional vectors (Clontech). HeLa-tTA cells that had been transfected with the bidirectional constructs were further selected under treatment with G418 to obtain stable lines and were referred to as BiFC cells. For YFP-based BiFC, YC (amino acids 159–240) and YN (amino acid 1–158) were used. The linker sequence used was 5′-GGTAGTGGTAGTGGTAGT-3′.

Immunoprecipitation, immunofluorescence and ChIP assays

Subcellular fractionation was performed according to the GeneTex protocol (http://www.genetex.com/Web/Protocol/Protocols.aspx) with several necessary changes. The nuclear fraction obtained was incubated with the appropriate antibody and protein A/G beads to enrich for target proteins. The bead-bound proteins were then eluted and subjected to immunoblotting. Band intensities were quantified by using ImageJ software (Schneider et al., 2012).

Immunofluorescence was performed as described previously (Liang et al., 2011).

ChIP assays were performed as described previously (Yochum et al., 2007) with minor modifications. The β-catenin antibody (9562), mouse TCF4 antibody (2953), normal Rabbit IgG (2729) and mouse IgG (5415) were purchased from Cell Signaling Technology. Unlabeled goat anti-rabbit IgG (01-15-06, KPL) was used in the β-catenin ChIP. All precipitated DNA was quantified by using real-time PCR. Data are presented as the percentage of input.

Flow cytometry and apoptosis assay

HCT116 cells were synchronized by using 2 mM thymidine (Sigma) for 20 h and were then released into fresh medium. FACS analysis was performed on a BD FACS Calibur instrument (BD Biosciences). Cell sorting was performed using a BD FACS Aria III instrument (BD Biosciences). Data were further analyzed by using ModFit and FlowJo. FITC staining of phosphorylated histone 3 was performed as described previously (Widrow and Laird, 2000). The apoptosis level was detected using the Apo-One Homogenous Caspase-3/7 kit (Promega).

RNA isolation, reverse transcription and real-time PCR

Total RNA was isolated with EZ-10 DNAaway RNA Mini-Preps Kit (BS88133, Sangon Biotech), and cDNA was generated using the Reverse Transcription System (Promega). Nascent RNA capture was performed using the Click-iT Nascent RNA capture Kit (Invitrogen).

ChIP-enriched DNA fragments and cDNA were analyzed by using real-time PCR on an ABI StepOne Plus instrument (Life Technologies). Primer sequences are listed in supplementary material Table S7.

Wnt target gene list and bioinformatics

The Wnt target gene list was prepared through an extensive review of published papers and resources including The Wnt Homepage (http://Wnt.stanford.edu). For details, see supplementary material Table S1. Gene annotation was performed using DAVID (http://david.abcc.ncifcrf.gov/).

Acknowledgements

We thank Randall T. Moon (University of Washington, Seattle, WA), Xi He (Harvard University, Boston, MA) and Chuanmao Zhang (School of Life Sciences of Peking University, Beijing, China) for supplying reagents. We also thank Hai Qi, Xiaohua Shen, Lei Huang, Meng Qing, Jinyu Wang, Guanhua Su, Yuan Li, Fangfang Li, Yanjian Li, Songpeng Zu, Weiwei Ma and Yue Wu for technical support (Tsinghua University, Beijing, China), as well as Guangwei Xin (School of Life Sciences of Peking University, Beijing, China), Guoliang Chai and Yi Ding (Tsinghua University, Beijing, China) for helpful discussions and suggestions.

Competing interests

The authors declare no competing interests.

Author contributions

Y.D. and S.S. performed most of the experiments and analyzed the data with contributions from X.Z., G.Z. and J.L. W.T. and S.C. were involved in BiFC construction. W.Wei suggested the use of and provided the Tet and pBI systems. Y.G. and L.L. synthesized the stapled peptide aStAx-35R. Y.G.C. and W.Wu supervised the study; and Y.D., S.S. and W.Wu wrote the manuscript.

Funding

This work was supported by grants to W.Wu from the National Natural Science Foundation of China [grant numbers 31471314, 81272235 and 30921004]; and the Major Science Programs of China [grant number 2011CB943803].

Supplementary material

Supplementary material available online at
http://jcs.biologists.org/lookup/suppl/doi:10.1242/jcs.146977/-/DC1

References

Abdullah, L. N. and Chow, E. K. (2013). Mechanisms of chemoresistance in cancer stem cells. *Clin. Transl. Med.* **2**, 3.

Aoki, K., Aoki, M., Sugai, M., Harada, N., Miyoshi, H., Tsukamoto, T., Mizoshita, T., Tatematsu, M., Seno, H., Chiba, T. et al. (2007). Chromosomal instability by beta-catenin/TCF transcription in APC or beta-catenin mutant cells. *Oncogene* **26**, 3511-3520.

Baron, U., Freundlieb, S., Gossen, M. and Bujard, H. (1995). Co-regulation of two gene activities by tetracycline via a bidirectional promoter. *Nucleic Acids Res.* **23**, 3605-3606.

Bartek, J., Lukas, C. and Lukas, J. (2004). Checking on DNA damage in S phase. *Nat. Rev. Mol. Cell Biol.* **5**, 792-804.

Batlle, E., Henderson, J. T., Beghtel, H., van den Born, M. M., Sancho, E., Huls, G., Meeldijk, J., Robertson, J., van de Wetering, M., Pawson, T. et al. (2002). Beta-catenin and TCF mediate cell positioning in the intestinal epithelium by controlling the expression of EphB/ephrinB. *Cell* **111**, 251-263.

Bilic, J., Huang, Y. L., Davidson, G., Zimmermann, T., Cruciat, C. M., Bienz, M. and Niehrs, C. (2007). Wnt induces LRP6 signalosomes and promotes dishevelled-dependent LRP6 phosphorylation. *Science* **316**, 1619-1622.
Cadigan, K. M. and Waterman, M. L. (2012). TCF/LEFs and Wnt signaling in the nucleus. *Cold Spring Harb. Perspect. Biol.* **4**, a007906.
Chen, S., Guttridge, D. C., You, Z., Zhang, Z., Fribley, A., Mayo, M. W., Kitajewski, J. and Wang, C. Y. (2001). Wnt-1 signaling inhibits apoptosis by activating beta-catenin/T cell factor-mediated transcription. *J. Cell Biol.* **152**, 87-96.
Chikazawa, N., Tanaka, H., Tasaka, T., Nakamura, M., Tanaka, M., Onishi, H. and Katano, M. (2010). Inhibition of Wnt signaling pathway decreases chemotherapy-resistant side-population colon cancer cells. *Anticancer Res.* **30**, 2041-2048.
Chilov, D., Sinjushina, N., Rita, H., Taketo, M. M., Mäkelä, T. P. and Partanen, J. (2011). Phosphorylated β-catenin localizes to centrosomes of neuronal progenitors and is required for cell polarity and neurogenesis in developing midbrain. *Dev. Biol.* **357**, 259-268.
Clevers, H. (2006). Wnt/beta-catenin signaling in development and disease. *Cell* **127**, 469-480.
Clevers, H. and Nusse, R. (2012). Wnt/β-catenin signaling and disease. *Cell* **149**, 1192-1205.
Dalton, S. (2013). G1 compartmentalization and cell fate coordination. *Cell* **155**, 13-14.
Davidson, G., Shen, J., Huang, Y. L., Su, Y., Karaulanov, E., Bartscherer, K., Hassler, C., Stannek, P., Boutros, M. and Niehrs, C. (2009). Cell cycle control of wnt receptor activation. *Dev. Cell* **17**, 788-799.
de Lau, W., Barker, N., Low, T. Y., Koo, B. K., Li, V. S., Teunissen, H., Kujala, P., Haegebarth, A., Peters, P. J., van de Wetering, M. et al. (2011). Lgr5 homologues associate with Wnt receptors and mediate R-spondin signalling. *Nature* **476**, 293-297.
DiNardo, S., Sher, E., Heemskerk-Jongens, J., Kassis, J. A. and O'Farrell, P. H. (1988). Two-tiered regulation of spatially patterned engrailed gene expression during Drosophila embryogenesis. *Nature* **332**, 604-609.
Elghazi, L., Gould, A. P., Weiss, A. J., Barker, D. J., Callaghan, J., Opland, D., Myers, M., Cras-Méneur, C. and Bernal-Mizrachi, E. (2012). Importance of β-Catenin in glucose and energy homeostasis. *Sci. Rep.* **2**, 693.
Gao, C., Xiao, G. and Hu, J. (2014). Regulation of Wnt/beta-catenin signaling by posttranslational modifications. *Cell Biosci.* **4**, 13.
Glinka, A., Dolde, C., Kirsch, N., Huang, Y. L., Kazanskaya, O., Ingelfinger, D., Boutros, M., Cruciat, C. M. and Niehrs, C. (2011). LGR4 and LGR5 are R-spondin receptors mediating Wnt/β-catenin and Wnt/PCP signalling. *EMBO Rep.* **12**, 1055-1061.
Goga, A., Yang, D., Tward, A. D., Morgan, D. O. and Bishop, J. M. (2007). Inhibition of CDK1 as a potential therapy for tumors over-expressing MYC. *Nat. Med.* **13**, 820-827.
Gonsalves, F. C., Klein, K., Carson, B. B., Katz, S., Ekas, L. A., Evans, S., Nagourney, R., Cardozo, T., Brown, A. M. and DasGupta, R. (2011). An RNAi-based chemical genetic screen identifies three small-molecule inhibitors of the Wnt/wingless signaling pathway. *Proc. Natl. Acad. Sci. USA* **108**, 5954-5963.
Graham, T. A., Weaver, C., Mao, F., Kimelman, D. and Xu, W. (2000). Crystal structure of a beta-catenin/Tcf complex. *Cell* **103**, 885-896.
Gregorieff, A. and Clevers, H. (2005). Wnt signaling in the intestinal epithelium: from endoderm to cancer. *Genes Dev.* **19**, 877-890.
Grossmann, T. N., Yeh, J. T., Bowman, B. R., Chu, Q., Moellering, R. E. and Verdine, G. L. (2012). Inhibition of oncogenic Wnt signaling through direct targeting of β-catenin. *Proc. Natl. Acad. Sci. USA* **109**, 17942-17947.
Hadjihannas, M. V., Brückner, M. and Behrens, J. (2010). Conductin/axin2 and Wnt signalling regulates centrosome cohesion. *EMBO Rep.* **11**, 317-324.
Hadjihannas, M. V., Bernkopf, D. B., Brückner, M. and Behrens, J. (2012). Cell cycle control of Wnt/β-catenin signalling by conductin/axin2 through CDC20. *EMBO Rep.* **13**, 347-354.
Hernandez, J. M., Farma, J. M., Coppola, D., Hakam, A., Fulp, W. J., Chen, D. T., Siegel, E. M., Yeatman, T. J. and Shibata, D. (2011). Expression of the antiapoptotic protein survivin in colon cancer. *Clin. Colorectal Cancer* **10**, 188-193.
Huang, X., Halicka, H. D., Traganos, F., Tanaka, T., Kurose, A. and Darzynkiewicz, Z. (2005). Cytometric assessment of DNA damage in relation to cell cycle phase and apoptosis. *Cell Prolif.* **38**, 223-243.
Huang, M., Wang, Y., Sun, D., Zhu, H., Yin, Y., Zhang, W., Yang, S., Quan, L., Bai, J., Wang, S. et al. (2006). Identification of genes regulated by Wnt/beta-catenin pathway and involved in apoptosis via microarray analysis. *BMC Cancer* **6**, 221.
Huang, P., Senga, T. and Hamaguchi, M. (2007). A novel role of phospho-beta-catenin in microtubule regrowth at centrosome. *Oncogene* **26**, 4357-4371.
Kerppola, T. K. (2006). Design and implementation of bimolecular fluorescence complementation (BiFC) assays for the visualization of protein interactions in living cells. *Nat. Protoc.* **1**, 1278-1286.
Khan, N. I. and Bendall, L. J. (2006). Role of WNT signaling in normal and malignant hematopoiesis. *Histol. Histopathol.* **21**, 761-774.
Kim, K., Pang, K. M., Evans, M. and Hay, E. D. (2000). Overexpression of beta-catenin induces apoptosis independent of its transactivation function with LEF-1 or the involvement of major G1 cell cycle regulators. *Mol. Biol. Cell* **11**, 3509-3523.
Kim, S. E., Huang, H., Zhao, M., Zhang, X., Zhang, A., Semonov, M. V., MacDonald, B. T., Zhang, X., Garcia Abreu, J., Peng, L. et al. (2013). Wnt stabilization of β-catenin reveals principles for morphogen receptor-scaffold assemblies. *Science* **340**, 867-870.
Klaus, A. and Birchmeier, W. (2008). Wnt signalling and its impact on development and cancer. *Nat. Rev. Cancer* **8**, 387-398.
Korinek, V., Barker, N., Morin, P. J., van Wichen, D., de Weger, R., Kinzler, K. W., Vogelstein, B. and Clevers, H. (1997). Constitutive transcriptional activation by a beta-catenin-Tcf complex in APC-/- colon carcinoma. *Science* **275**, 1784-1787.
Lee, E., Salic, A. and Kirschner, M. W. (2001). Physiological regulation of [beta]-catenin stability by Tcf3 and CK1epsilon. *J. Cell Biol.* **154**, 983-994.
Lee, G., White, L. S., Hurov, K. E., Stappenbeck, T. S. and Piwnica-Worms, H. (2009). Response of small intestinal epithelial cells to acute disruption of cell division through CDC25 deletion. *Proc. Natl. Acad. Sci. USA* **106**, 4701-4706.
Lento, W., Congdon, K., Voermans, C., Kritzik, M. and Reya, T. (2013). Wnt signaling in normal and malignant hematopoiesis. *Cold Spring Harb. Perspect. Biol.* **5**, a008011.
Leow, P. C., Tian, Q., Ong, Z. Y., Yang, Z. and Ee, P. L. (2010). Antitumor activity of natural compounds, curcumin and PKF118-310, as Wnt/β-catenin antagonists against human osteosarcoma cells. *Invest. New Drugs* **28**, 766-782.
Li, V. S., Ng, S. S., Boersema, P. J., Low, T. Y., Karthaus, W. R., Gerlach, J. P., Mohammed, S., Heck, A. J., Maurice, M. M., Mahmoudi, T. et al. (2012). Wnt signaling through inhibition of β-catenin degradation in an intact Axin1 complex. *Cell* **149**, 1245-1256.
Liang, J., Fu, Y., Cruciat, C. M., Jia, S., Wang, Y., Tong, Z., Tao, Q., Ingelfinger, D., Boutros, M., Meng, A. et al. (2011). Transmembrane protein 198 promotes LRP6 phosphorylation and Wnt signaling activation. *Mol. Cell. Biol.* **31**, 2577-2590.
Lindqvist, A., Källström, H., Lundgren, A., Barsoum, E. and Rosenthal, C. K. (2005). Cdc25B cooperates with Cdc25A to induce mitosis but has a unique role in activating cyclin B1-Cdk1 at the centrosome. *J. Cell Biol.* **171**, 35-45.
Liu, Q. and Ruderman, J. V. (2006). Aurora A, mitotic entry, and spindle bipolarity. *Proc. Natl. Acad. Sci. USA* **103**, 5811-5816.
Logan, C. Y. and Nusse, R. (2004). The Wnt signaling pathway in development and disease. *Annu. Rev. Cell Dev. Biol.* **20**, 781-810.
MacDonald, B. T., Tamai, K. and He, X. (2009). Wnt/beta-catenin signaling: components, mechanisms, and diseases. *Dev. Cell* **17**, 9-26.
Mao, J., Wang, J., Liu, B., Pan, W., Farr, G. H., 3rd, Flynn, C., Yuan, H., Takada, S., Kimelman, D., Li, L. et al. (2001). Low-density lipoprotein receptor-related protein-5 binds to Axin and regulates the canonical Wnt signaling pathway. *Mol. Cell* **7**, 801-809.
Masckauchán, T. N., Shawber, C. J., Funahashi, Y., Li, C. M. and Kitajewski, J. (2005). Wnt/beta-catenin signaling induces proliferation, survival and interleukin-8 in human endothelial cells. *Angiogenesis* **8**, 43-51.
Minard, M. E., Ellis, L. M. and Gallick, G. E. (2006). Tiam1 regulates cell adhesion, migration and apoptosis in colon tumor cells. *Clin. Exp. Metastasis* **23**, 301-313.
Moon, R. T., Kohn, A. D., De Ferrari, G. V. and Kaykas, A. (2004). WNT and beta-catenin signalling: diseases and therapies. *Nat. Rev. Genet.* **5**, 691-701.
Najdi, R., Syed, A., Arce, L., Theisen, H., Ting, J. H., Atcha, F., Nguyen, A. V., Martinez, M., Holcombe, R. F., Edwards, R. A. et al. (2009). A Wnt kinase network alters nuclear localization of TCF-1 in colon cancer. *Oncogene* **28**, 4133-4146.
Niehrs, C. and Acebron, S. P. (2012). Mitotic and mitogenic Wnt signalling. *EMBO J.* **31**, 2705-2713.
Norbury, C., Blow, J. and Nurse, P. (1991). Regulatory phosphorylation of the p34cdc2 protein kinase in vertebrates. *EMBO J.* **10**, 3321-3329.
Olmeda, D., Castel, S., Vilaró, S. and Cano, A. (2003). Beta-catenin regulation during the cell cycle: implications in G2/M and apoptosis. *Mol. Biol. Cell* **14**, 2844-2860.
Orford, K., Orford, C. C. and Byers, S. W. (1999). Exogenous expression of beta-catenin regulates contact inhibition, anchorage-independent growth, anoikis, and radiation-induced cell cycle arrest. *J. Cell Biol.* **146**, 855-868.
Orsulic, S., Huber, O., Aberle, H., Arnold, S. and Kemler, R. (1999). E-cadherin binding prevents beta-catenin nuclear localization and beta-catenin/LEF-1-mediated transactivation. *J. Cell Sci.* **112**, 1237-1245.
Ouyang, H., Zhuo, Y. and Zhang, K. (2013). WNT signaling in stem cell differentiation and tumor formation. *J. Clin. Invest.* **123**, 1422-1424.
Pauklin, S. and Vallier, L. (2013). The cell-cycle state of stem cells determines cell fate propensity. *Cell* **155**, 135-147.
Pećina-Šlaus, N. (2010). Wnt signal transduction pathway and apoptosis: a review. *Cancer Cell Int.* **10**, 22.
Pei, Y., Brun, S. N., Markant, S. L., Lento, W., Gibson, P., Taketo, M. M., Giovannini, M., Gilbertson, R. J. and Wechsler-Reya, R. J. (2012). WNT signaling increases proliferation and impairs differentiation of stem cells in the developing cerebellum. *Development* **139**, 1724-1733.
Penelova, A., Richman, L., Neupert, B., Simanis, V. and Kühn, L. C. (2005). Analysis of the contribution of changes in mRNA stability to the changes in steady-state levels of cyclin mRNA in the mammalian cell cycle. *FEBS J.* **272**, 5217-5229.
Rabbitts, P. H., Watson, J. V., Lamond, A., Forster, A., Stinson, M. A., Evan, G., Fischer, W., Atherton, E., Sheppard, R. and Rabbitts, T. H. (1985). Metabolism of c-myc gene products: c-myc mRNA and protein expression in the cell cycle. *EMBO J.* **4**, 2009-2015.
Rao, T. P. and Kühl, M. (2010). An updated overview on Wnt signaling pathways: a prelude for more. *Circ. Res.* **106**, 1798-1806.

Journal of Cell Science

Resnitzky, D., Gossen, M., Bujard, H. and Reed, S. I. (1994). Acceleration of the G1/S phase transition by expression of cyclins D1 and E with an inducible system. *Mol. Cell. Biol.* **14**, 1669-1679.
Rulifson, I. C., Karnik, S. K., Heiser, P. W., ten Berge, D., Chen, H., Gu, X., Taketo, M. M., Nusse, R., Hebrok, M. and Kim, S. K. (2007). Wnt signaling regulates pancreatic beta cell proliferation. *Proc. Natl. Acad. Sci. USA* **104**, 6247-6252.
Schneider, C. A., Rasband, W. S. and Eliceiri, K. W. (2012). NIH Image to ImageJ: 25 years of image analysis. *Nat. Methods* **9**, 671-675.
Schweinfest, C. W., Fujiwara, S., Lau, L. F. and Papas, T. S. (1988). c-myc can induce expression of G0/G1 transition genes. *Mol. Cell. Biol.* **8**, 3080-3087.
Sekiya, T., Nakamura, T., Kazuki, Y., Oshimura, M., Kohu, K., Tago, K., Ohwada, S. and Akiyama, T. (2002). Overexpression of Icat induces G(2) arrest and cell death in tumor cell mutants for adenomatous polyposis coli, beta-catenin, or Axin. *Cancer Res.* **62**, 3322-3326.
Shan, B. E., Wang, M. X. and Li, R. Q. (2009). Quercetin inhibit human SW480 colon cancer growth in association with inhibition of cyclin D1 and survivin expression through Wnt/beta-catenin signaling pathway. *Cancer Invest.* **27**, 604-612.
Shyu, Y. J., Liu, H., Deng, X. and Hu, C. D. (2006). Identification of new fluorescent protein fragments for bimolecular fluorescence complementation analysis under physiological conditions. *Biotechniques* **40**, 61-66.
Stamos, J. L. and Weis, W. I. (2013). The β-catenin destruction complex. *Cold Spring Harb. Perspect. Biol.* **5**, a007898.
Valenta, T., Hausmann, G. and Basler, K. (2012). The many faces and functions of β-catenin. *EMBO J.* **31**, 2714-2736.
van de Wetering, M., Sancho, E., Verweij, C., de Lau, W., Oving, I., Hurlstone, A., van der Horn, K., Batlle, E., Coudreuse, D., Haramis, A. P. et al. (2002). The beta-catenin/TCF-4 complex imposes a crypt progenitor phenotype on colorectal cancer cells. *Cell* **111**, 241-250.
Vaziri, S. A., Hill, J., Chikamori, K., Grabowski, D. R., Takigawa, N., Chawla-Sarkar, M., Rybicki, L. R., Gudkov, A. V., Mekhail, T., Bukowski, R. M. et al. (2005). Sensitization of DNA damage-induced apoptosis by the proteasome inhibitor PS-341 is p53 dependent and involves target proteins 14-3-3sigma and survivin. *Mol. Cancer Ther.* **4**, 1880-1890.
Vijayakumar, S., Liu, G., Rus, I. A., Yao, S., Chen, Y., Akiri, G., Grumolato, L. and Aaronson, S. A. (2011). High-frequency canonical Wnt activation in multiple sarcoma subtypes drives proliferation through a TCF/β-catenin target gene, CDC25A. *Cancer Cell* **19**, 601-612.
Vlad, A., Röhrs, S., Klein-Hitpass, L. and Müller, O. (2008). The first five years of the Wnt targetome. *Cell. Signal.* **20**, 795-802.
Widrow, R. J. and Laird, C. D. (2000). Enrichment for submitotic cell populations using flow cytometry. *Cytometry* **39**, 126-130.
Yochum, G. S., McWeeney, S., Rajaraman, V., Cleland, R., Peters, S. and Goodman, R. H. (2007). Serial analysis of chromatin occupancy identifies beta-catenin target genes in colorectal carcinoma cells. *Proc. Natl. Acad. Sci. USA* **104**, 3324-3329.
You, Z., Saims, D., Chen, S., Zhang, Z., Guttridge, D. C., Guan, K. L., MacDougald, O. A., Brown, A. M., Evan, G., Kitajewski, J. et al. (2002). Wnt signaling promotes oncogenic transformation by inhibiting c-Myc-induced apoptosis. *J. Cell Biol.* **157**, 429-440.
Yuan, D., Liu, L. and Gu, D. (2007). Transcriptional regulation of livin by beta-catenin/TCF signaling in human lung cancer cell lines. *Mol. Cell. Biochem.* **306**, 171-178.
Zeng, X., Tamai, K., Doble, B., Li, S., Huang, H., Habas, R., Okamura, H., Woodgett, J. and He, X. (2005). A dual-kinase mechanism for Wnt co-receptor phosphorylation and activation. *Nature* **438**, 873-877.
Zhang, T., Otevrel, T., Gao, Z., Gao, Z., Ehrlich, S. M., Fields, J. Z. and Boman, B. M. (2001). Evidence that APC regulates survivin expression: a possible mechanism contributing to the stem cell origin of colon cancer. *Cancer Res.* **61**, 8664-8667.
Zhu, G., Wang, Y., Huang, B., Liang, J., Ding, Y., Xu, A. and Wu, W. (2012). A Rac1/PAK1 cascade controls β-catenin activation in colon cancer cells. *Oncogene* **31**, 1001-1012.
Zimmerman, Z. F., Kulikauskas, R. M., Bomsztyk, K., Moon, R. T. and Chien, A. J. (2013). Activation of Wnt/β-catenin signaling increases apoptosis in melanoma cells treated with trail. *PLoS ONE* **8**, e69593.

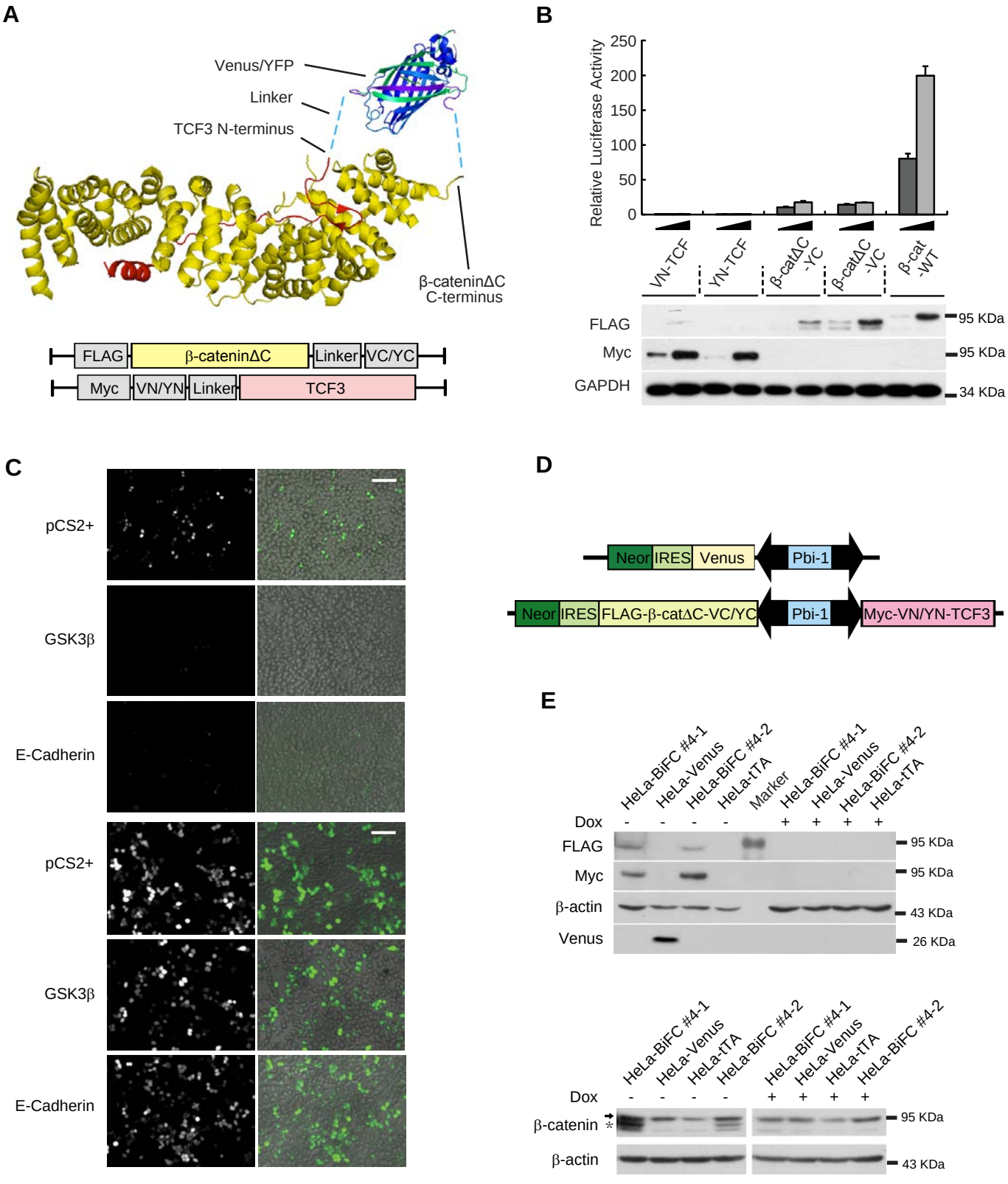
A
Venus/YFP
Linker
TCF3 N-terminus
β-cateninΔC
C-terminus
FLAG
β-cateninΔC
Linker
VC/YC
Myc
VN/YN
Linker
TCF3
B
Relative Luciferase Activity
250
200
150
100
50
0
VN-TCF
YN-TCF
β-catΔC -YC
β-catΔC -VC
β-cat -WT
FLAG
Myc
GAPDH
95 KDa
95 KDa
34 KDa
C
pCS2+
GSK3β
E-Cadherin
pCS2+
GSK3β
E-Cadherin
D
Neor
IRES
Venus
Pbi-1
Neor
IRES
FLAG-β-catΔC-VC/YC
Pbi-1
Myc-VN/YN-TCF3
E
HeLa-BiFC #4-1
HeLa-Venus
HeLa-BiFC #4-2
HeLa-tTA
Marker
HeLa-BiFC #4-1
HeLa-Venus
HeLa-BiFC #4-2
HeLa-tTA
Dox
- - - - + + + +
FLAG
Myc
β-actin
Venus
95 KDa
95 KDa
43 KDa
26 KDa
HeLa-BiFC #4-1
HeLa-Venus
HeLa-tTA
HeLa-BiFC #4-2
HeLa-BiFC #4-1
HeLa-Venus
HeLa-tTA
HeLa-BiFC #4-2
Dox
- - - - + + + +
β-catenin
*
β-actin
95 KDa
43 KDa

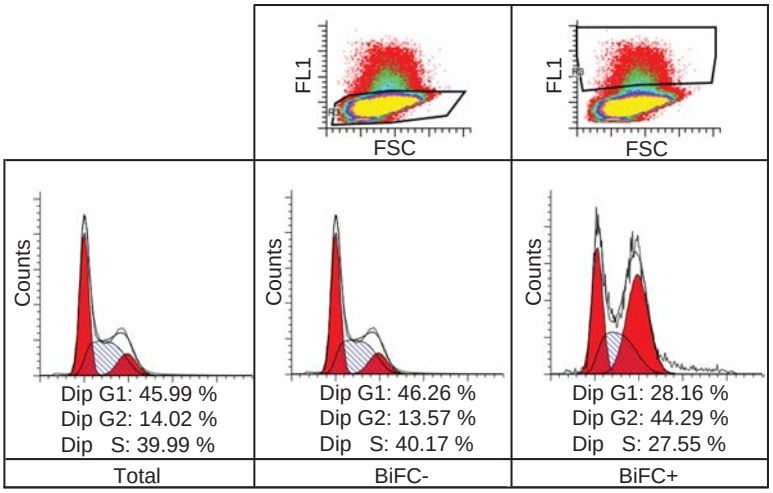
FL1
FSC
FL1
FSC
Counts
Dip G1: 45.99 %
Dip G2: 14.02 %
Dip S: 39.99 %
Total
Counts
Dip G1: 46.26 %
Dip G2: 13.57 %
Dip S: 40.17 %
BiFC-
Counts
Dip G1: 28.16 %
Dip G2: 44.29 %
Dip S: 27.55 %
BiFC+

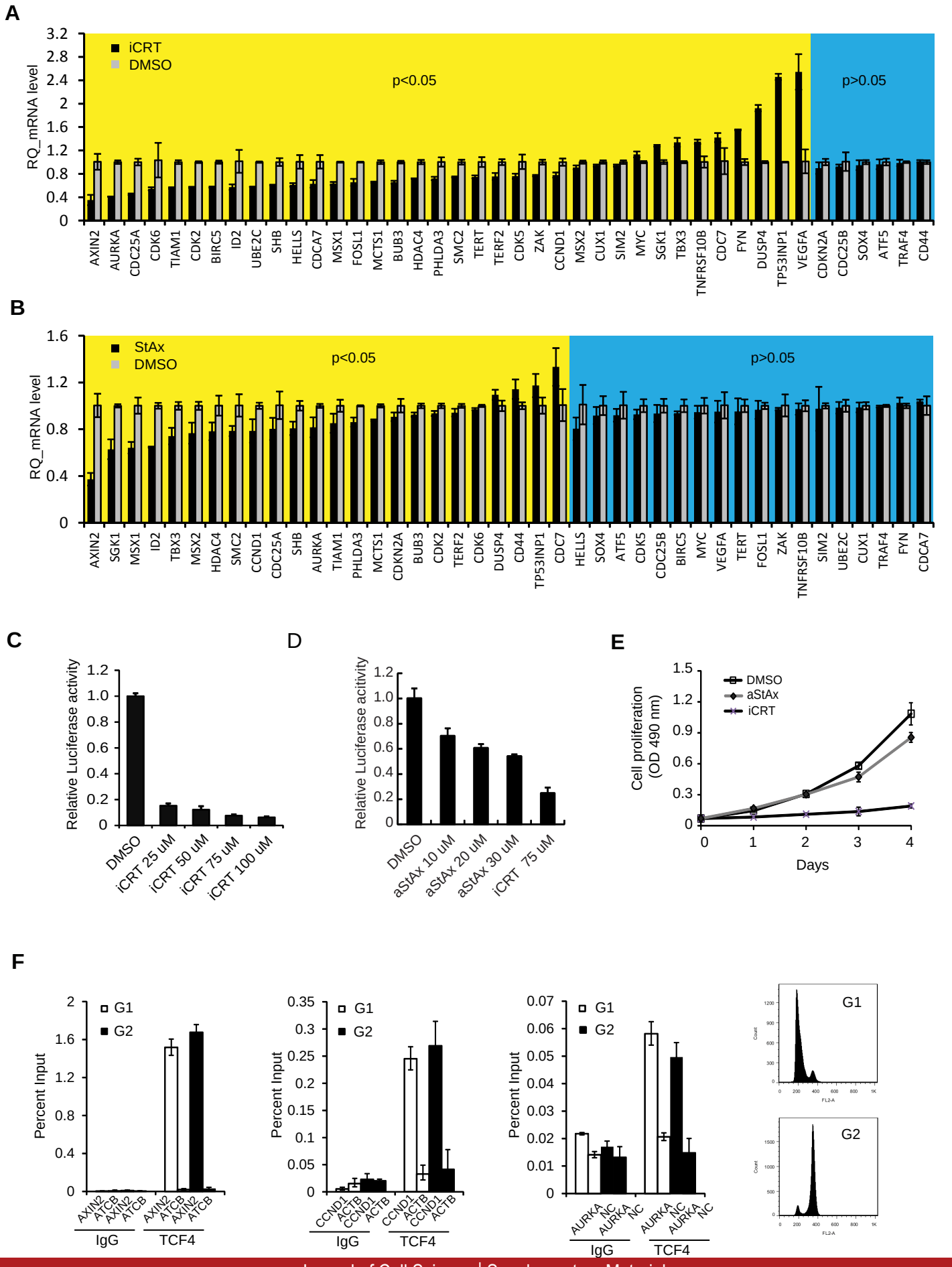
A
RQ_mRNA level
iCRT
DMSO
p<0.05
p>0.05
AXIN2 AURKA CDC25A CDK6 TIAM1 CDK2 BIRC5 ID2 UBE2C SHB HELLS CDCA7 MSX1 FOSL1 MCTS1 BUB3 HDAC4 PHLDA3 SMC2 TERT TERF2 CDK5 ZAK CCND1 MSX2 CUX1 SIM2 MYC SGK1 TBX3 TNFRSF10B CDC7 FYN DUSP4 TP53INP1 VEGFA CDKN2A CDC25B SOX4 ATF5 TRAF4 CD44
B
RQ_mRNA level
StAx
DMSO
p<0.05
p>0.05
AXIN2 SGK1 MSX1 ID2 TBX3 MSX2 HDAC4 SMC2 CCND1 CDC25A SHB AURKA TIAM1 PHLDA3 MCTS1 CDKN2A BUB3 CDK2 TERF2 CDK6 DUSP4 CD44 TP53INP1 CDC7 HELLS SOX4 ATF5 CDK5 CDC25B BIRC5 MYC VEGFA TERT FOSL1 ZAK TNFRSF10B SIM2 UBE2C CUX1 TRAF4 FYN CDCA7
C
Relative Luciferase activity
DMSO
iCRT 25 uM
iCRT 50 uM
iCRT 75 uM
iCRT 100 uM
D
Relative Luciferase acitivity
DMSO
aStAx 10 uM
aStAx 20 uM
aStAx 30 uM
iCRT 75 uM
E
Cell proliferation (OD 490 nm)
DMSO
aStAx
iCRT
Days
F
Percent Input
G1
G2
AXIN2 ACTB AXIN2 ACTB AXIN2 ACTB AXIN2 ACTB
IgG
TCF4
CCND1 ACTB CCND1 ACTB CCND1 ACTB CCND1 ACTB
IgG
TCF4
AURKA NC AURKA NC AURKA NC AURKA NC
IgG
TCF4
G1
G2

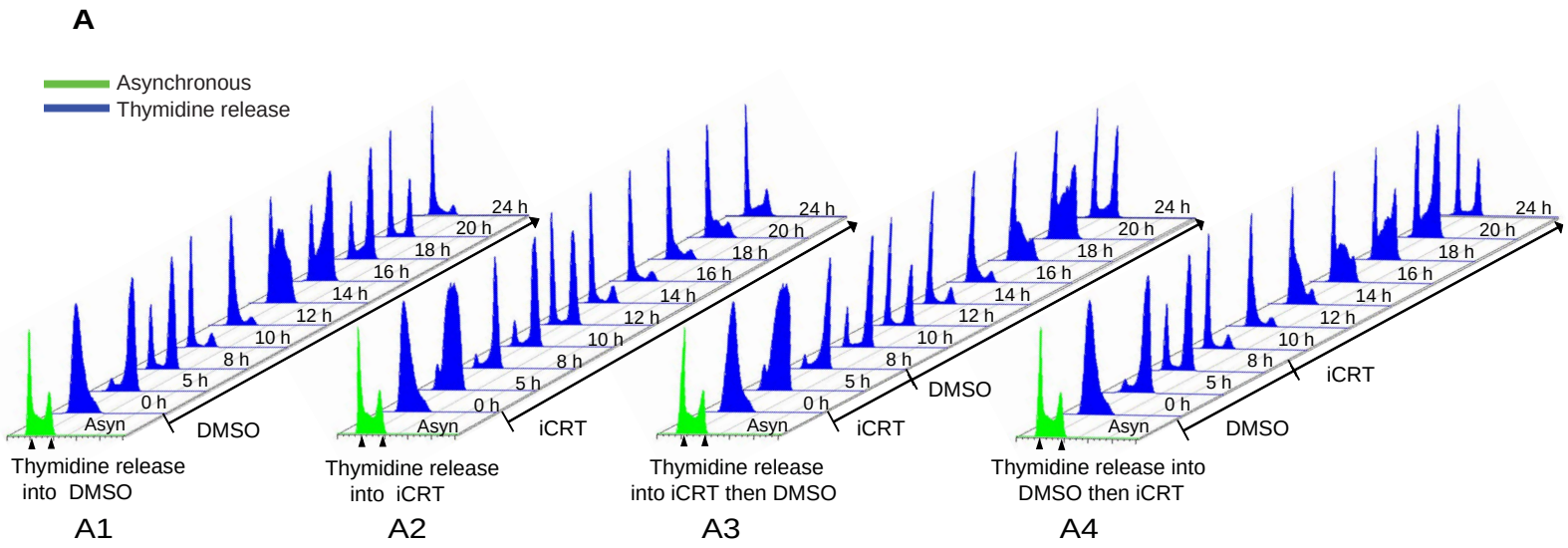
A
Asynchronous
Thymidine release
Asyn
0 h
5 h
8 h
10 h
12 h
14 h
16 h
18 h
20 h
24 h
DMSO
iCRT
Thymidine release into DMSO
Thymidine release into iCRT
Thymidine release into iCRT then DMSO
Thymidine release into DMSO then iCRT
A1
A2
A3
A4

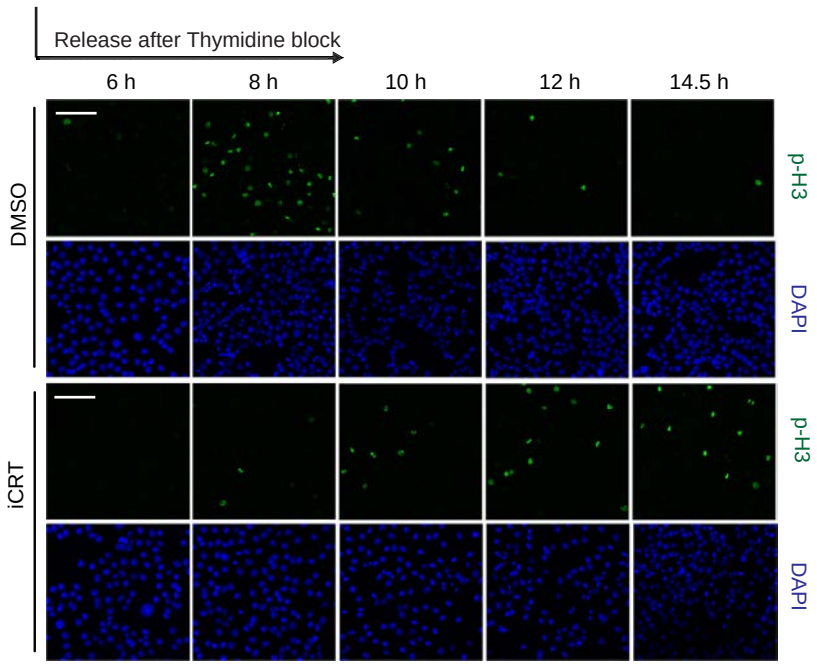
B
Release after Thymidine block
6 h
8 h
10 h
12 h
14.5 h
DMSO
iCRT
p-H3
DAPI

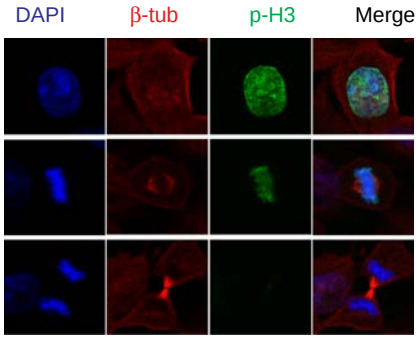
C
DAPI
β-tub
p-H3
Merge

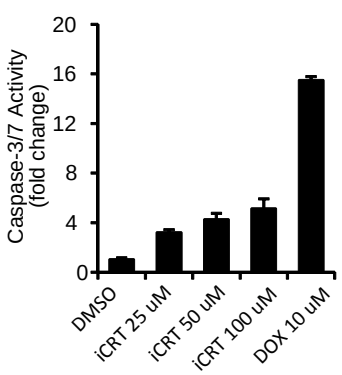
D
Caspase-3/7 Activity (fold change)
0
4
8
12
16
20
DMSO
iCRT 25 uM
iCRT 50 uM
iCRT 100 uM
DOX 10 uM

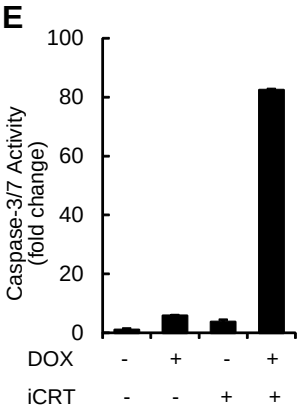
E
Caspase-3/7 Activity (fold change)
0
20
40
60
80
100
DOX - + - +
iCRT - - + +

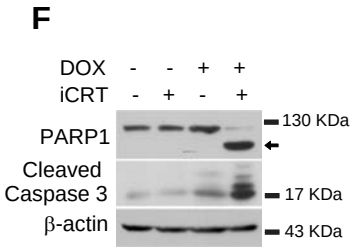
F
DOX - - + +
iCRT - + - +
PARP1
Cleaved Caspase 3
β-actin
130 KDa
17 KDa
43 KDa

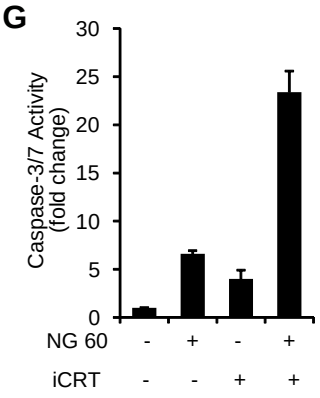
G
Caspase-3/7 Activity (fold change)
0
5
10
15
20
25
30
NG 60 - + - +
iCRT - - + +

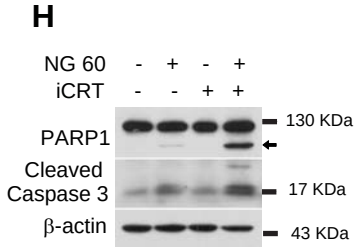
H
NG 60 - + - +
iCRT - - + +
PARP1
Cleaved Caspase 3
β-actin
130 KDa
17 KDa
43 KDa

Supplementary Figure legends

Fig. S1. Visualization of the β-catenin/TCF complex by BiFC.

A. Top: Schematic of the BiFC biosensor. The BiFC biosensor comprises β-catenin (yellow) and TCF3 (red) proteins, each was fused with a half of Venus protein (VC and VN) or YFP protein (YC and YN) at their C- and N-terminus, respectively. Bottom: Schematic of the BiFC constructs. FLAG or Myc tag was added at their N-terminus for protein detection. A C-terminal deleted β-catenin (β-catenin ΔC) was used in all cases to minimize the Wnt activity when these constructs were over-expressed.

B. Top: Wnt-responsive TOP-FLASH reporter assay in HEK293T cells transfected with BiFC components. Five or ten ng plasmid DNA per well in 96 well plate were transfected, respectively. Bottom: The expression levels of the BiFC components in these samples were determined by Western blot. FLAG antibody was used to detect FLAG-β-cateninΔC-VC/YC and Myc antibody was used to detect Myc-VN/YN-TCF3. GAPDH was used as a loading control.

C. BiFC signals (upper panels) or GFP signals (lower panels) in HEK293T cells after co-transfection with the indicated plasmids. Fluorescence and phase-contrast merged fluorescence images are shown. Bar = 100 μm.

D. Schematic of the constructs for the doxycycline-repressible BiFC stable lines. The pBI vector allows the simultaneous regulation of both β-cat-VC and VN-TCF3 by one central, bidirectional TRE (Tet responsive element). The internal ribosome entry site (IRES) permits the translation of two open reading frames from one messenger RNA. These constructs were introduced into HeLa-tTA cells to produce stable cell lines. A doxycycline-repressible Venus stable line was also established as a control.

E. Western blot analysis of the expression levels of the biosensor components and Venus in doxycycline-repressible BiFC and Venus stable cell lines. Withdraw of Dox (doxycycline) induced the expression of the proteins. The relative expression level was compared in lower panel, which indicated that the β-cat-VC (*) was at a similar

level to endogenous β-catenin (arrow). Since the C-terminal domain of β-catenin was deleted, it is still slightly smaller than the wild type, even though it is fused to half of the Venus protein (VC).

Fig. S2. The β-catenin/TCF BiFC signal accumulates during the S-G2 phases.

Analysis of the DNA content profile and YFP signal intensity of BiFC-YFP stable cells by flow cytometry. The BiFC-YFP signal could only be detected after incubation for 4 h at 30℃. The cells were then fixed by paraformaldehyde, stained with propidium iodide and analyzed by FACS. The DNA content profiles of the total, BiFC-positive, and -negative gated populations are shown.

Fig. S3. Identification of β-catenin/TCF target genes during the S-G2 phases.

A, B. Effects on Wnt target genes expression in S-G2 phase HCT116 cells upon Wnt inhibition by (A) iCRT or (B) aStAx . HCT116 cells were synchronized and treated as in Fig. 3B. Forty two genes in the cell death and cell cycle categories were analyzed using real-time PCR. The results are the average of triplicate data; the SD and p-values were calculated in a two-tailed student t-test.

C. Wnt-responsive TOP-FLASH reporter assay in HCT116 cells with the indicated treatments. iCRT or vehicle was introduced 24 h before cell lysis and detection.

D. Wnt-responsive TOP-FLASH reporter assay in HCT116 cells to compare the inhibitory effects of aStAx and iCRT. iCRT, aStAx, or vehicle was introduced 24 h before cell lysis and detection.

E. MTT assay in HCT116 cells to compare the inhibitory effect of aStAx and iCRT on cell proliferation. The cells were treated with DMSO, iCRT (50 μM) or aStAx (20 μM) for 4 days and the MTT assay was performed every day. The results presented are the mean ± SD from quintuplicate samples.

F. Chromatin immunoprecipitation assays in G2- or G1-enriched HCT116 cells (5 h and 12.5 h after release from the thymidine block, using TCF4 or a mouse IgG antibodies as indicated. Promoter regions of *AXIN2*, *CCND1* and *AURKA* were tested

and the promoter of ACTB (β-actin) was used as a control. All graphs show the average with SD (n = 3). The cell cycle status is also shown.

Fig. S4. β-catenin/TCF complex-mediated target gene expression ensures G2/M progression and cell survival.

A. Delay of cell cycle progression by iCRT treatment. Synchronized HCT116 cells were released into medium containing either DMSO (control) or 75 μM iCRT. (A1) DMSO; (A2) iCRT; (A3) iCRT for the first 8 h and then replaced by DMSO containing medium; (A4) DMSO for the first 9 h and then replaced by iCRT containing medium. Cells were harvested at the indicated time points and their cellular DNA content was determined by propidium iodide staining and flow cytometry. Asyn, asynchronous cells.

B. HCT116 cells after release from a thymidine block were treated with DMSO or iCRT for the indicated time periods and then fixed and stained with p-H3 antibody (green) or DAPI (blue). Bar = 100 μm.

C. Closer views of representative iCRT-treated HCT116 cells at different stages of mitosis. Cells were stained with DAPI (blue), p-H3 (green) or β-tubulin (β-tub, red). Bar = 10 μm.

D. Caspase-3/7 activation in response to Wnt inhibition by iCRT. HCT116 cells were incubated with DMSO, iCRT or DOX (Doxorubicin, as a positive control) for 24 h. Effects on Caspase-3/7 activity were assessed using the Apo-ONE homogeneous Caspase-3/7 assay. Results show the fold increase of Caspase-3/7 activity relative to the DMSO-treated cells. Each data point represents the mean ± SD of the experiment performed in triplicate.

E, F. Sensitivity of iCRT-treated (50 μM) HCT116 cells to Doxorubicin-triggered (DOX, 1 μM) apoptosis. Cells were treated for 24 h. Apoptosis was detected by measurement of (E) Caspase-3/7 activity and (F) cleavage of Caspase-3 and PARP1 by Western blot. The arrow indicates the cleaved PARP1.

G, H. Sensitivity of iCRT-treated (50 μM) HCT116 cells to NG 60-triggered (7.5 μM) apoptosis. Cells were treated for 24 h. Apoptosis was detected by measurement of (G)

caspase-3/7 activity and (H) cleavage of Caspase-3 and PARP1 by Western blot. The arrow indicates the cleaved PARP1.

Movie 1: Example 1 of a dynamic β-catenin/TCF-BiFC signal during the cell cycle. HeLa cells expressing the BiFC biosensor were traced for 40 h. Images were recorded every 30 min by a high content screening platform (HCS, ArrayScan VTI 700, ThermoFisher Cellomics).

Movie 2: Example 2 of a dynamic β-catenin/TCF-BiFC signal during the cell cycle. HeLa cells expressing the BiFC biosensor were traced for 40 h. Images were recorded by HCS platform.

Movie 3: HeLa cells expressing the BiFC biosensor were released from a thymidine block and then traced for 26 h. Images were recorded every 20 min by a Nikon Ti-E A1Rsi inverted confocal microscope (Nikon Instruments).

Movie 4: Example 1 of a Venus fluorescence signal during the cell cycle. HeLa cells expressing the Venus fluorescence proteins were traced for 40 h. Images were recorded by HCS platform.

Movie 5: Example 2 of a Venus fluorescence signal during the cell cycle. HeLa cells expressing the Venus fluorescence proteins were traced for 40 h. Images were recorded by HCS platform.

Movie 1.

Movie 2.

Movie 3.

Movie 4.

Movie 5.

Tables S1 to S7.

Download Supplementary Tables